PHASED ARRAY ANTENNA CALIBRATION AND EXPERIMENTAL VALIDATION

A THESIS SUBMITTED TO
THE GRADUATE SCHOOL OF NATURAL AND APPLIED SCIENCES
OF
MIDDLE EAST TECHNICAL UNIVERSITY

BY

ALPER YALIM

IN PARTIAL FULFILLMENT OF THE REQUIREMENTS
FOR
THE DEGREE OF MASTER OF SCIENCE
IN
ELECTRICAL AND ELECTRONICS ENGINEERING

MARCH 2013

Approval of the Thesis

"PHASED ARRAY ANTENNA CALIBRATION AND EXPERIMENTAL VALIDATION"

Submitted by **ALPER YALIM** in partial fulfillment of the requirements for the degree of **Master of Science in Electrical and Electronics Engineering** by,

Prof. Dr. Canan Özgen

Dean, Graduate School of **Natural and Applied Sciences** _______________

Prof. Dr. İsmet Erkmen

Head of Department, **Electrical and Electronics Engineering Dept.** ______________

Prof. Dr. Şimşek Demir

Supervisor, **Electrical and Electronics Engineering Dept., METU** _______________

Examining Committee Members

Prof. Dr. Gülbin Dural
Electrical and Electronics Engineering Dept., METU _______________

Prof. Dr. Şimşek Demir
Electrical and Electronics Engineering Dept., METU _______________

Prof. Dr. Özlem Aydın Çivi
Electrical and Electronics Engineering Dept., METU _______________

Assoc. Prof. Dr. Lale Alatan
Electrical and Electronics Engineering Dept., METU _______________

Mehmet Erim İnal
Electrical and Electronics Engineering, ASELSAN _______________

Date: 27.03.2013

I hereby declare that all information in this document has been obtained and presented in accordance with academic rules and ethical conduct. I also declare that, as required by these rules and conduct, I have fully cited and referenced all material and results that are not original to this work.

Name, Lastname : Alper Yalım

Signature :

ABSTRACT

CALIBRATION OF THE PHASED ARRAY ANTENNAS

Yalım, Alper
M.S., Department of Electrical and Electronics Engineering
Supervisor: Prof. Dr. Şimşek Demir

March 2013, 54 pages

In this thesis, nine different methods aiming calibration of Phased Array Antenna (PAA) and Multifunctional Radars which employ PAA are presented. Those calibration methods are described, procedures of the methods are explained in detail, and information about constraints and measurement restrictions of those methods is given. As one step further, comprehensive work is focused on Multi-Element Phase Toggling (MEP) method and Rotating Element Vector (REV) method. Results of simulations are shown, theoretical and practical aspects of calibration methods are analytically elaborated. MEP and REV methods are experimentally implemented on a phased array receiver. Results of indoor and outdoor measurements are also presented in the scope of this thesis.

Keywords: Phased Array Antenna, Multifunctional Radar, Multi-Element Phase Toggling method, Rotating Element Vector method.

ÖZ

FAZ DİZİLİ ANTEN KALİBRASYONU

Yalım, Alper
Yüksek Lisans, Elektrik ve Elektronik Mühendisliği Bölümü
Tez Yöneticisi: Prof. Dr. Şimşek Demir

Mart 2013, 54 sayfa

Bu tezde Faz Dizili Antenler ve bu tip antenler kullanılarak oluşturulan Çok Fonksiyonlu Radarlar (Multifunctional Radar) için kullanılması muhtemel kalibrasyon metodları hakkında yapılan araştırmanın sonucu olan dokuz yöntem yer almaktadır. Bahsedilen dokuz kalibrasyon metodu tanıtılmış, metodların prosedürleri ayrıntılı bir şekilde anlatılmıştır ve yine bu kalibrasyon yollarının kısıtlamaları, ölçüm limitleri hakkında bilgiler verilmiştir. Bir ileri adımda, Multi-Element Phase Toggling (MEP) metodu ve Rotating Element Vector (REV) metoduna yoğunlaşmış kapsamlı çalışmalar yer almıştır. Bu metodlarla ilgili simulasyon sonuçları listelenmiş, teori ve uygulama temelleri analitik olarak ortaya konulmuştur. MEP ve REV metodları faz dizili anten kullanan bir alıcı kullanılarak deneysel olarak uygulanmıştır.

Anahtar Kelimeler: Faz Dizili Antenler, Çok Fonksiyonlu Radarlar, Çoklu Eleman Faz Değiştirme metodu, Çevirilen Eleman Vektoru metodu.

To My family,

ACKNOWLEDGEMENTS

I would like to express my gratitude to my supervisor Assoc. Prof. Dr. Şimşek Demir for his guidance, suggestions and support throughout research.

I would like to thank Çağrı Çetintepe, Özgehan Kılıç and Yusuf Sevinç for their contribution to the thesis and support.

I would like to thank my friends in METU Antenna and Microwave Laboratory for such friendly research environments they had provided.

Finally, I would like to thank my family for their love, support and trust to me.

TABLE OF CONTENTS

LIST OF TABLES

TABLES

LIST OF FIGURES

FIGURES

CHAPTER 1

INTRODUCTION

Control on the shape of radiation beam provides exact designation of maximum radiation points and nulls, reduces unintended side lobe levels while increasing resistance to interference or jamming activities. Moreover, accurate rotation of the radiation beam to the desired point enables performing of operation with less power since radiated energy only illuminates the required region. Therefore, beam shaping and beam steering are very important subjects in efficient, secure electromagnetic applications.

There are four ways used for switching beams, namely; mechanical rotation, frequency scanning, putting time delay between array elements and providing progressive phase distributions between elements. Frequency is a sensitive operation parameter to choose for steering the beam and in frequency scan, there is not enough intervention points to calibrate the system due to the nature of the system since there is no control elements such as phase shifters, attenuators, vector modulators located to control each element separately. Time delaying method is independent from the frequency but time delaying circuitries should be placed to each element which is not practical in terms of many aspects such as complexity, cost and feasibility. One of the remaining two ways is mechanical rotation which has mechanical limits; not adequately fast and reliability of mechanic system is vulnerable to exposing problems. Mechanical rotation is infeasible to shaping radiation pattern or varying parameters of radiation. Moreover, in the mechanical rotation, the calibration is limited to mechanical imperfections. The phase scanning seems to be more acceptable beam steering method in terms of operation capability, speed and reliability. Multitasks can be performed at the same time by the use of the phase scanning using aperture sharing or time scheduling. Therefore, Phased Array Antenna which uses phase scanning is a hot topic to develop superior radar systems.

The Phased Array Antenna (PAA) contains elements each of which has a phase shifter. Beams are formed by the help of relative phase differences given to elements of the array. Freedom of choosing weightings in terms of amplitude and phase provides an electronically adjustable radiation pattern. The coverage is limited to a 120 degree sector, but in that sector, high gain with low side lobe levels, arbitrary modes of surveillance and tracking can be achieved. Additionally, even if a single component reduces or loses capability, the system remains operational. Another important feature of PAAs, multifunction operation can be performed by emitting several beams simultaneously. Therefore, the phased array concept is the most prevalent example of the array concept and it constitutes the fundamental building block of many modern radar and communication systems enabling multifunctional and adaptive processing.

Conventional radars consist of a rotating transmitter and sensor, perform only one function with separate units required for surveillance, tracking and targeting; however, multifunctional radars can be deployed with electronically scanned antennas and fully multifunctional radars use Active Electronically Scanned Arrays (AESA), which contain a transmit-receive channel (T/R) for each radiator. Multifunctionality may also be achieved by mechanical scanning to some extent; however, there is a fact that the multifunctionality is really facilitated by AESAs. The advantages of AESA are fast adaptive beam shaping, agility, improved power efficiency, improved mode interleaving, simultaneous multiple weapon support, and reduced detectability.

So far, advantages and importance of phased array radar are explained. On the other hand, the complexity of the phased array radar concept causes some problems which can affect performance of the operation considerably. Therefore, one of the important challenges of making the phased array radar is removing all kind of mismatches, distortions and losses inherent within the system [1]. For a radar application, the portion of the space illuminated by the radar beam must be predicted with high accuracy although unstable operation parameters exist. There are many reasons of loss or distortion in a radar system. Connector losses, cabling losses or mismatches can make identical elements behave differently which causes unwanted side lobe levels and reduces the radiated or received power. Other problems caused by mutual coupling effects or surface waves reduce power, they may also change the pattern of the radiation and may cause blind points. All of these effects are strictly unacceptable for a radar system. Therefore, wide variety of error sources gives calibration of the radar much importance and so this thesis.

The calibration can be implemented to the system by the help of external antennas or probes located in front of the array or in the plane of the array to measure over all effects including mutual coupling and scattering from nearby structure of the antenna. Calibration can also be implemented with couplers, passive or active calibration units which are embedded to the system locating behind of radiators, at the input or output of the Transmit/Receive (TR) modules or in the beam forming network.

In this thesis, nine different methods intended for calibration of Phased Array Radar systems are introduced and implementation procedures of calibration methods are explained by simulations and applications. Advantageous and weak aspects of methods are discussed.

Two methods, namely; Multi Element Phase Toggling (MEP) method [1]-[8] and Rotating Element Vector (REV) method [11]-[17] are found applicable since these two methods come into prominence in terms of accuracy, time efficiency, requiring less complexity and adaptation capability to the operational environment. Furthermore, MEP and REV methods can be applied to large arrays since these methods aim to get radiated energy from the whole array.

Following the describing section of the nine methods, selected two methods are explained. Detailed implementation procedures of measurements performed for MEP, REV methods and results of measurements are interpreted in the scope of this thesis.

Moreover, in this thesis, answers to the question that how REV and MEP methods can be applied to the large scale arrays and what can be done to improve cited calibration methods are looked for. An iterative way for the REV procedure which simplifies the implementation of the REV procedure and removes the need of using large reference signals will be introduced in the procedure of the REV method part.

1.1 ORGANIZATION OF THE THESIS

This thesis aims to provide the findings from an in-depth literature survey on phased array antenna calibration techniques and to support these findings with simulation as well as measurement results for a selected subset of those calibration methods. In accordance with this goal;

Chapter-2 covers definition and importance of calibration in phased array systems. Moreover, information about sources of error in radar systems is given. Brief descriptions of nine calibration methods in the literature are given in Chapter-2.

Chapter-3 explains procedures of MEP and REV methods in detail and gives simulation results performed for those selected methods by the use of MATLAB® software. Illustrative figures are generated for extraction of the weighting coefficients for each element using implemented calibration method.

Chapter-4 describes the experimental set-up. Array configuration, propagation paths of channels and outputs of receiver system are introduced as well as operation parameters of the system. Operation constraints and limits of the set-up are stated. Moreover, Chapter-4 gives experimental results of the REV and MEP methods. Experiments are performed using the experimental phased array antenna receiver set-up and indoor and outdoor measurements are taken. There are also different implementations of the REV method to improve the classical REV method and results are compared with each other.

Chapter-5 includes the conclusion of the thesis and the thesis ends with references part.

CHAPTER 2

CALIBRATION AND CALIBRATION METHODS

Phased arrays are widely used in military applications which expect high performance from the antennas, such as low side lobes and narrow beamwidth. Degradation in this performance may severely affect the success of operation. For instance, satellite communication requires high directivity with low sidelobe levels [24]. The distortion in this radiation pattern may require higher transmit power or cause interference to neighboring satellites or receivers. Similar comments can be also stated for the phased array radars, for which the portion of the space illuminated by the radar beam must be predicted with high accuracy to resist jamming and to perform proper targeting, surveillance and tracking. At this point, the calibration and quality of the calibration become important.

Calibration, in general sense, can be defined as eliminating or minimizing systematic factors that negatively affect the performance of the system. On the other hand, calibration of a phased array antenna may be defined as forcing each element of the array to behave in an identical manner. If all elements exhibit the same element factor, array theory can be implemented easily by adjusting excitation coefficients of elements by considering the desired array factor.

In the following parts, possible error sources of Phased Array Radar systems and intervention points to the system for calibration will be discussed.

2.1 ERROR SOURCES

In general, errors can be divided into three main categories, namely, random errors, drift errors and systematic errors.

Random errors cannot be modeled due to their random characteristics. Therefore, these errors cannot be eliminated, but their effect may be decreased by increasing the observation time and increasing the number of measurements which is equivalent to averaging. Indeed, this type of errors is out of scope of calibration in the operation environment.

Drift errors correspond to variations in performances and characteristics of components in comparatively long term. The drift errors mainly occur due to temperature and aging. Effects of the drift errors could be minimized by instrumental calibration.

Finally, the systematic errors cover all other errors which show the same effect on consecutively repeated measurements; there is stability in systematic error terms. Periodic implementations of the PAA calibration in the operational environment aim to get rid of this type of errors.

There are several error sources affecting the performance of a phased array. Some examples about the most important error sources can be useful to explain functions of calibration methods.

For instance, in a phased array, individual antenna elements are excited with desired complex coefficients. These coefficients can be imposed in the form of in-phase and quadrature components. Phase and gain imbalance between in-phase (I) and quadrature (Q) branches of each element causes unbalanced weighting of the elements and therefore causes nonidentical radiation characteristics of array elements. I and Q paths' bias errors due to electronic DC offsets, co-channel gain and phase errors can be listed as the error sources of individual elements.

In an array there are a number of elements, and in most of the cases, there are many active and passive components connected to individual elements. Therefore, in addition to the distortions of individual elements, interactions, which can be named as coupling, among the antenna elements become unavoidable. Those interactions among different elements and also between components of the same channel generate uncertainty over radar illumination and that kind of uncertainty causes a major problem for proper operation by causing failed tasks. This mutual coupling has to be characterized to remove undesired effects such as gain reduction, unintended changes in the angle of maximum radiation and unexpected nulls in the radiation beam. The mutual coupling includes not only coupling between radiators but also coupling between signal channels and components in the background electronics behind antennas due to inadequate isolation.

Another source of uncertainty in the phased array operation may be the physical location errors or performance loss of radiating elements at the front-end structure. Since the radiation part of the radar is exposed to environmental effects such as bird droppings, rain, and snow, the radiation pattern can be affected negatively.

Scattering by antenna mounting structure or other nearby structures, for example the body of the ship and the masts, can also be a problem for radar operation and calibration is also expected to identify and remove these scattering effects.

Moreover, one of the most important error sources has to be mentioned in this subsection is temperature. Specially, characteristics of active components can change considerably due to the temperature.

To sum up, error sources can be due to several factors including changes in environmental conditions, mechanical variations, assembly inaccuracies, mutual coupling effects, mistuned or failed amplifiers and phase shifters such that one or several bits of phase shifters can become invalid and amplitude errors can be reasoned from not excited elements.

2.2 CALIBRATION

Calibration can be divided into two main categories according to place where calibration is employed. The first is the factory calibration which is performed at the fabrication stage only once. As the factory calibration, PAA is usually measured in an anechoic chamber and aligned in a near field range. In this stage, an external receiving probe is positioned in front of each radiating element. Amplitude and phase of each element are measured and aligned appropriately. The second is in-field calibration or with other name 'in-situ' calibration. As can be understood from its name, in-field calibration is performed while the radar system is operating in activation environment. In-field calibration is performed at regular intervals throughout the life of the array. The aim of the in-field calibration is removing destructive effects of system losses, identifying antenna elements, network imperfections or faults, keeping the radar system performance well as much as possible.

Although details and extent of calibration vary from system to system, virtually all of radar calibration methods require that each element's amplitude, phase or time delay are set correctly to achieve desired beam pattern. Calibration can be performed by using different topologies. The calibration antenna specifications are highly related with the topology to be chosen, the calibration methods will be classified under three main topics:

1) calibration using external antennas,

2) calibration using mutual coupling of array elements with internal elements or probes,
3) calibration using an embedded special designed network.

The first topic is realizing calibration by the help of an external antenna element which is used as a transmitter or receiver. External elements can be located at the far field, radiating near field or at the plane of the array.

An external antenna may be undesirable due to the possible distortion of the field pattern caused by the probe and its mechanical structure in the boresight of the array, and it may also be inconvenient in the space-limited applications like airborne. The Second topic includes making calibration by placing external probes at the periphery of the array or using internal elements of the array. Locating probes at the periphery of the array is preferred since the flexibility of the array design can be conserved, and additional coupling effects due to the probe can be avoided. However it should be concluded that only small-sized arrays can be calibrated by such a configuration, at most 8 by 8 elements seem to be calibrated in this fashion. This calibration configuration is indeed used in systems utilizing small arrays such as mobile satellite communication systems, or airborne radar systems. Therefore, methods utilizing mutual-coupling between the array elements are also used in the PAA calibration systems. Mutual-coupling based methods can be used in large arrays differently from probe-based uniplanar counterparts.

In the third topic, calibration is made by the help of additional couplers. A test signal is injected into the channels of the array from the beamformer input and it propagates through transmission lines and electrical components and finally calibration unit via couplers or directly network analyzer port instead of radiator. This process can be realized vice versa by giving test signal from radiator part and receiving from beam former input. Unlike using external antennas, in the case of embedded designed network, measured electromagnetic waves propagate along the transmission lines instead of propagating along free space.

The questionable point about the calibration is how an influence can be made to the system during existence of an error. Since calibration aims to keep the system operational, some non-ideal effects such as mutual coupling between elements, phase differences or losses due to transmission path lengths, small losses of wave energy and undesired characteristics of electronic components can be compensated with changes in weightings of array elements to make elements behave in identical manners. This intervention can be made by the help of phase shifters or attenuators of individual channels of the array. If the error cannot be compensated with the change in weightings or if there is a distortion in any component such a case of fully or partly loss of performance, the calibration will propose altering the related component.

2.3 CALIBRATION METHODS IN LITERATURE

There are several methods about calibration of phased array radars in the literature [1]-[31]. These methods can also be expanded by employing different kinds of probe antennas which can be located in the near field, mid-field or far field of the array. Some methods are very convenient for small arrays and some are suitable in the use for large scale arrays. Therefore, array size can be a factor to choose appropriate calibration method. Some calibration methods can be done in small time intervals, however, some methods take much time according to their contents of implementation procedures. Time consumption is important concern, but it should not be overlooked that there is a trade-off between time consumption and accuracy.

The following section provides insight for calibration methods available in the literature. There are nine calibration methods in this part to be described.

2.3.1 MULTI-ELEMENT PHASE TOGGLING (MEP) METHOD

Multi-element phase toggling method aims to calibrate groups of elements simultaneously [1]. Therefore, total signals from elements of the array are measured according to the specific phase settings implemented to each element. Specific phase settings are used to identify elements while extracting correction coefficients for element excitations after completing the measurements.

For identifying elements, MEP method uses the Fourier properties of the beamformer by changing the phase shifter states 0° to 360° of each individual element with specialized phase steps. The method is based on measurements of received signals from any array, phase states of whose individual elements are rotated step by step in a specified manner. A pick-up antenna is required and all elements in the array should have individual phase shifters to implement MEP method. Moreover, elements must have such phase shifters that phase increments between successive phase steps are stable in the cycle of phase rotation.

In the MEP method, Fourier Transform is implemented to the measured signals. The method aims to acquire weighting coefficients of array elements in the Fourier spectrum corresponding to their phase change steps. DC point at Fourier spectrum corresponds to the contribution of the fixed components from the environment and also includes the effect of elements in a large array whose phase states have not been altered during measurements.

Different references suggest far field measurements for the MEP method and under this condition the method gives exact results. In fact, the MEP method can be also used with measurements in the near field of the array if the distance from the array is far enough to get the radiated power from the whole array.

MEP method is one of the selected methods and the procedure of this method will be explained in detail in Chapter-3.

2.3.2 MID-FIELD CALIBRATION TECHNIQUE OF PHASED ARRAY ANTENNAS

Mid-Field Calibration method is an in-field method. As illustrated in **Figure 1**, horizontal part denotes a linear array and there are two fixed radiators in front of the array at a distance equal to the antenna inter-element spacing in the array. The signals transmitted from those radiators are received by two adjacent elements of the array. The method uses the ratio of these received signals and recursively multiplies these ratios and so, all elements excitation coefficients relation are acquired with respect to a reference antenna excitation value.

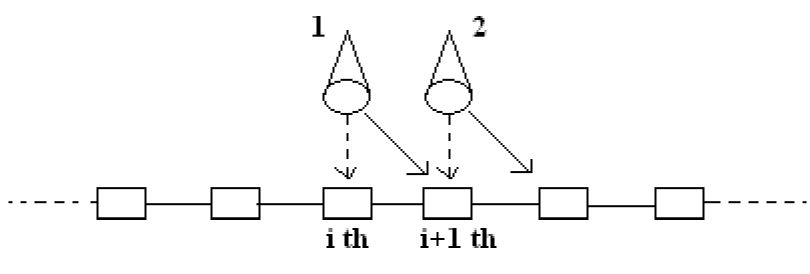

Figure 1. Configuration for the mid-field calibration technique.

The title of "mid-field calibration" comes from the location of radiators such that radiators are in the far field of an individual element, but near field when the whole array is considered [9].

In **Figure 2**, the procedure of the mid-field calibration technique is shown with a block diagram to explain the method.

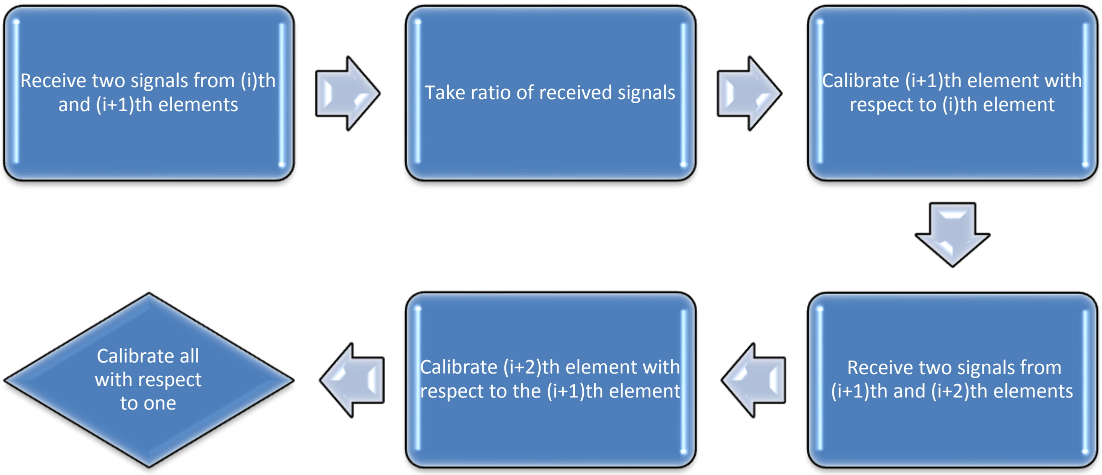

Figure 2. Configuration for the mid-field calibration technique.

The method basically uses the idea that signals transmitted from two adjacent radiators are received by two adjacent elements of the array through identical paths. In [9], it is stated that due to the equality of directivities for same angle and identical propagation paths, received signal ratio from two radiators for i^{th} and $(\mathrm{i}+1)^{\mathrm{th}}$ reduces to excitation values of i^{th} and $(\mathrm{i}+1)^{\mathrm{th}}$ elements, respectively I_i and I_{i+1};

$$S_{i+1}^{rad2}/\, S_i^{rad1} = I_{i+1}/\, I_i \tag{2.1}$$

Using the ratio of received signals, the method completely uses the recursive multiplication to get calibrate elements with respect to one of them. If the first element excitation value is taken as reference assigned as 1, the second element excitation value can be acquired by multiplying 1 × (received signal by second element for transmitting second radiator divided by received signal by first element for transmitting first radiator). Then, to find third element excitation value, multiply 1 × (second element received signal/first element received signal) × (third element received signal/second element received signal). Stating mathematically,

$$I_{i+2}/\, I_i = (S_{i+1}^{rad2}/\, S_i^{rad1})\, (S_{i+2}^{rad2}/\, S_{i+1}^{rad1}) \tag{2.2}$$

$$I_{i+3}/\, I_i = (S_{i+1}^{rad2}/\, S_i^{rad1})\, (S_{i+2}^{rad2}/\, S_{i+1}^{rad1})\, (S_{i+3}^{rad2}/\, S_{i+2}^{rad1}) \tag{2.3}$$

This method can be readily generalized to two dimensional arrays. In this case, at least three radiators are employed instead of two. First, explained procedure is applied to individual rows. The rows calculations are made by using radiator-1 and radiator-2. Then, a similar procedure is applied to the columns by using radiator-1 and radiator-3. After that, any row, column element can be found with respect to any element in the array by multiplying selected element column values with the ratio of the element corresponding to the selected column from reference element row value set.

2.3.3 A CALIBRATION TECHNIQUE EMPLOYING PASSIVE ELEMETS FOR CALIBRATION OF ACTIVE PHASED ARRAY ANTENNAS

In [10], a calibration technique for active phased array antennas that uses a small number of passive array elements dedicated to calibration is stated. The dedicated calibration elements are passive, meaning they do not have T/R modules behind them.

This proposed method aims to remove the disadvantages of employing external horns and the problem of internal coupling between transmit and receive chains of the T/R module. In external calibration element case, the array should be firstly aligned in the near-field range of the array and then mutual coupling between the horns and array elements are measured. These measurements become the factory standard for the array. Field calibration is accomplished by comparing mutual coupling measurements taken during deployment with the factory standard. Such a calibration technique employing external elements increases the effective array size footprint and increases antenna radar cross section (RCS). Furthermore, as the array size increases, the signal-to-noise ratio resulting from coupling between the external horns and central array elements may not be high enough to provide the required measurement accuracy for calibrating the array to the original state.

The proposed calibration method uses mutual coupling between a few dedicated internal passive elements and all active array elements. By using passive elements, the accuracy of mutual coupling measurements is increased significantly and separate transmit and receive beamformers are not required.

This method uses basically a mutual coupling based calibration technique employing a small number of passive calibration elements which are internal array elements. The passive calibration elements are directly connected to a calibration unit and so they do not share active array RF beamformers. Therefore, this calibration technique does not require high isolation between active array elements and does not increase the array footprint.

The calibration procedure can be explained as follows: Firstly, the array is divided into several blocks with a single passive calibration element located near the center of each block. A simple such division is depicted in **Figure 3**. The transmit signal from the calibration unit is routed by the switch network to a single passive calibration element. All other active elements in the array are turned off. Then a single element in a block adjacent to the selected passive calibration element block is tuned on to receive while others are still turned off. The transmit signal from the passive calibration element is received via mutual coupling by the active element under test. After this process is completed, the current active element is turned off and an adjacent active element in the same block is set to receive the calibration signal from the same passive calibration element. This process is repeated for every active array element in this block. When all the elements in the block are calibrated, the elements in other blocks adjacent to the passive calibration element block are calibrated. Then, a new passive calibration element (and so new block) is selected and the active elements in adjacent blocks of this new block are calibrated. Mentioned process continues until all active elements in the array are handled.

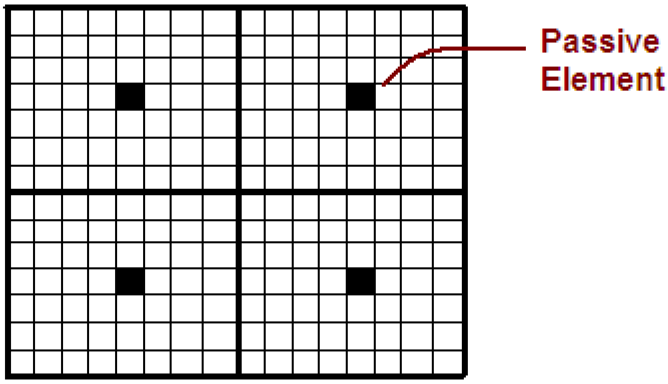

Figure 3. A sample partitioning of active array elements, passive calibration elements are indicated on the figure.

As an advantage of this method, all blocks can be calibrated by at least two passive calibration elements. Calibration of active elements using multiple passive calibration elements provides redundancy to protect the system if there is an unlikely failure of a passive calibration element.

In the factory and after the antenna is deployed in the field, the mutual coupling between calibration elements and array elements is measured in the same way. The mutual coupling data measured in the field are compared to the factory standard data.

The block size limit (and so number of passive calibration elements) is dependent on factors, namely; mutual coupling levels between the passive calibration element and the active element, low noise amplifier (LNA) and calibration unit transmit power. The calibration unit output power level should be chosen so that the farthest element in the adjacent block has sufficient coupling and the nearest LNA in the adjacent block is not saturated (stays in the linear region). Thus, the receiver sensitivity of the farthest active element in the adjacent block and LNA saturation level of the nearest active element in the adjacent block will determine the required minimum calibration unit output power and the maximum calibration block size in the array.

2.3.4 ROTATING ELECTRIC FIELD VECTOR (REV) METHOD

Rotating Electric Field Vector (REV) method can be used as a near-field method using near-field scanner probe or far-field method to get radiated energy from the whole antenna array to be calibrated.

REV method can be implemented to a single element of the array by the use of external probe which is located in front of that element while other elements of the array are turned-off. In such a configuration, the probe is in the near-field of the antenna array and the probe is mobile.

REV method can be implemented by the use of an external antenna which is located in the far-field and boresight of the array. In this configuration, the external antenna position is fixed and that antenna receives energy from the whole array or transmits energy to the whole array.

REV method measures the radiating electric field of each element antenna in a phased array. This measurement method takes the advantage of the fact that the combined power of the array antenna is sinusoidal when the excitation phase of a single element to be tested is varied from 0° to 360°. Relative amplitudes and relative phases of each element in terms of electric field vectors are extracted from sinusoidal power variation values with respect to a large, non-rotating reference [13]. If the phase of the tested element and the phase of the reference are in-phase, the measured power value will be maximum. If those phases are 180° different from each other, the measured power value corresponding to that instant will be minimum.

In **Figure 4**, measured power from the antenna array which is sinusoidal power measurement corresponding to the phase variation of an element is shown, offset value depicts contribution of the rest of the array and reference signal.

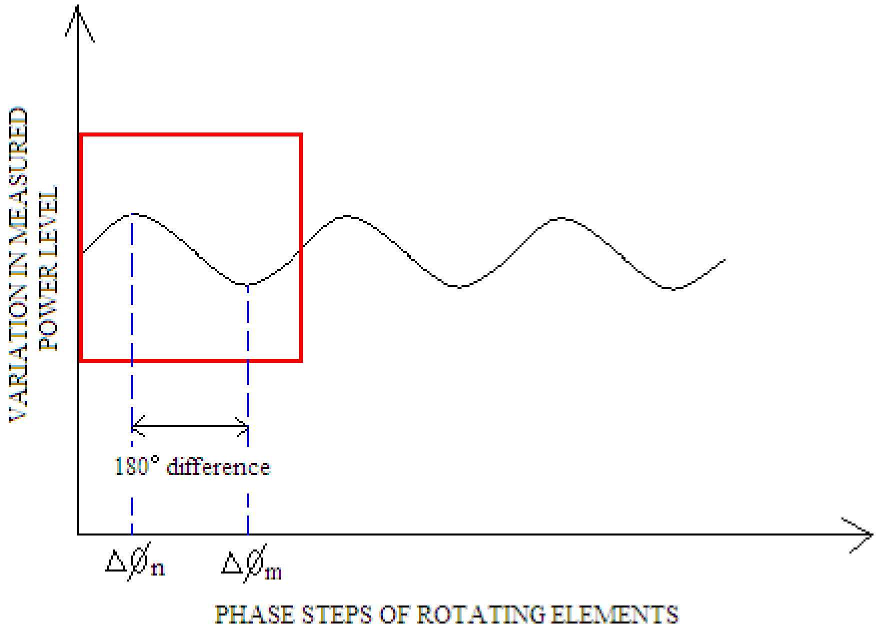

Figure 4. Measured sinusoidal power variation corresponding to phase steps

Figure 5 illustrates the basic principle of the REV method and demonstrates the “rotating vector” concept for a sample four-element linear array.

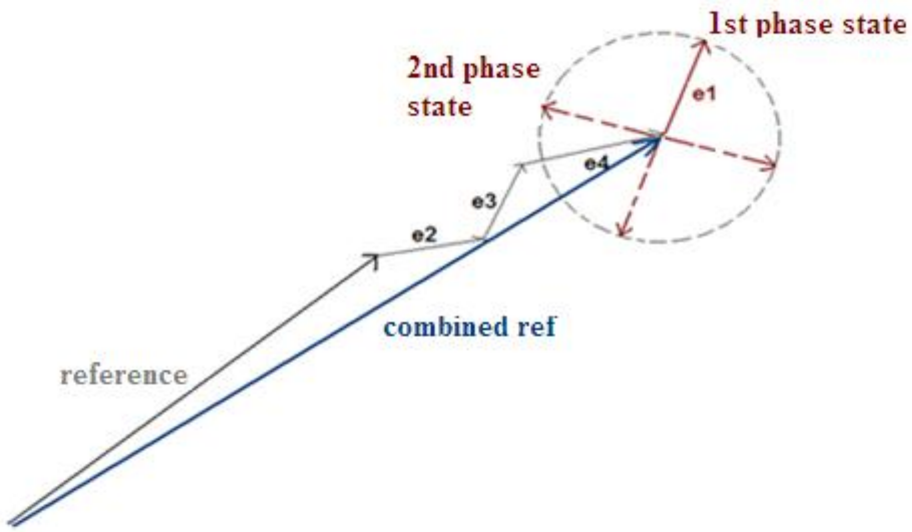

Figure 5. The principle of the REV method illustrated using phasors.

If a four-element linear array is assumed with a fixed internal or external reference to the antenna array to be calibrated, a sample configuration is illustrated in **Figure 5**. The Rotating phase state of the tested element corresponds to contribution vector e1 in **Figure 5**, while elements rather than the tested element, which are denoted by e2, e3 and e4, are in their initial phase states and contribution vector of all non-rotating elements is combined ref.

The novelty of REV method is that REV method calculates radiation vectors of each element from only measured power data. There is no need to the phase information in REV method. Non-essential phase information reduces complexity of calibration and makes REV method applicable.

The REV method is based on the element electric field measurement which includes all the effects such as mutual coupling between antenna elements, background structures and also scattering effects by ambient structural configurations.

The procedure and detailed explanation of the REV method will be clarified in Chapter-3.

2.3.5 COMBINED ROTATING ELECTRIC FIELD VECTOR (CREV) METHOD

The classic REV method can be in sufficient for large arrays since far elements' individual phase changes may not be observed from the pick-up antenna properly. The Combined REV (CREV) method seeks to overcome these limitations using a different approach over the classic REV; CREV method changes the phases of a *group* of elements by their phase shifters, as although signals transmitted by far elements are weak; received composite signals variation can be seen if a large number of far elements' phases are rotated synchronously. By doing so, the SNR ratio improves since measurements are made over a group of elements at a fixed position of the receiver. Moreover, this method with a fixed receiver reduces the coupling between the receiver and array elements [17].

The nearest elements to the probe are measured in the same way as the classic REV method; but the farther elements are divided into the different size clusters. The size of cluster increases if the distance from the receiver antenna increases. Considering a specific example can be helpful to understand the idea behind the CREV method. Assume that there is a linear array of ten elements. Linear array elements are divided into the three clusters as shown in **Figure 6**. The 1st element measurements are performed as the classic REV method. Second cluster measurements are performed in three steps: By (i) changing phase states of the 2nd, 3rd and 4th elements simultaneously, then (ii) only changing 2nd and 4th elements phase states at the same time, and (iii) only changing 2nd and 3rd elements phase states synchronously. The variations will give the element contributions after solving relevant equations. Third cluster includes more elements to achieve significant power variation from the furthest elements.

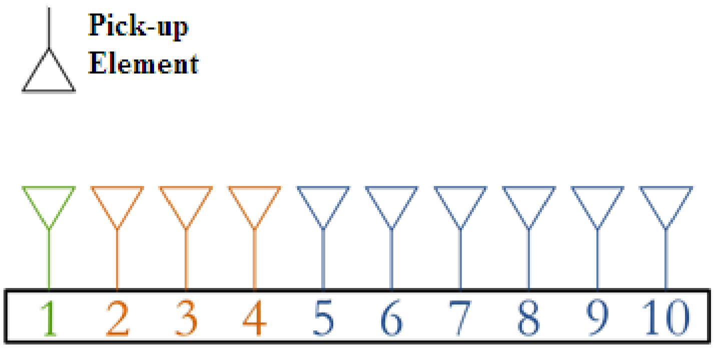

Figure 6. Calibration scheme for CREV method.

The CREV methodology is based on obtaining equations number of which is equal to the number of elements in the cluster. In **Figure 6**, there are three elements in the second cluster. Firstly, rotate phases of 2nd, 3rd and 4th elements simultaneously, resultant rotating vector which can be extracted by using classic REV algorithm will be combination of initial phase states of 2nd, 3rd and 4th elements including their phase offset errors. Resultant vector is denoted by $R_1$and excitation values of elements are denoted by Ex in the equation 2.4,

$$Ex_2 \exp(j\phi_2) + Ex_3 \exp(j\phi_3) + Ex_4 \exp(j\phi_4) = R_1 \tag{2.4}$$

After taking the first result of combined vector rotation, secondly, rotate phases of 2nd and 4th elements and resultant combined vector is denoted by R_2 in the equation 2.5,

$$Ex_2 \exp(j\phi_2) + Ex_4 \exp(j\phi_4) = R_2 \tag{2.5}$$

Final measurement set for the second cluster will be performed by rotating phases of 2nd and 3rd elements synchronously and resultant combined vector is denoted by R_3 in the equation 2.6,

$$Ex_2 \exp(j\phi_2) + Ex_3 \exp(j\phi_3) = R_3 \tag{2.6}$$

There are three equations and three unknowns after completing measurements for the second cluster. Therefore, values of individual elements can be found analytically.

2.3.6 LEAST SQUARE SOLUTION METHOD

Many algorithms in literature use the following multiplication form to model non-ideal effects on received voltages as,

$$b(\emptyset) = CZa(\emptyset) \tag{2.7}$$

Where $b(\emptyset)$ is an N by 1 vector of measured voltages received by an N element antenna array for signal incident from direction $\emptyset$, *C* is an N by N matrix representing variations of complex gain among antennas, feed lines and receivers; *Z* is an N by N matrix including mutual coupling between antenna elements and structure scattering effects, $a(\emptyset)$ is an N by 1 vector of ideal voltage values for direction $\emptyset$ which only depends on array geometry and individual element pattern. This method gives a least square formulation approach to find *Z* matrix.

The method assumes that there are only antenna effects, so *C* matrix can be assumed to be an identity matrix and therefore, previous equation reduces to the form [20],

$$b(\emptyset) = CZa(\emptyset) \quad \Rightarrow \quad b(\emptyset) = Za(\emptyset) \tag{2.8}$$

Here, the aim is finding the *Z* matrix, because if *Z* matrix is found, one can predict $b(\emptyset)$ for any angle $\emptyset$.

In order to find the *Z* matrix, firstly, k measurements from different directions (which are widely separated and not coincident with grating lobes) are needed to acquire B_k matrix (N by k) where N is the number of array elements. Then, one calculates ideal voltage values for these k directions and acquire A_k matrix (N by k). Now, equation is in the form of B_k = ZA_k, and finally, with the use of the Least Square solution for *Z* in [20]:

$$Z = B_k\, A_k^H\, (A_k\, A_k^H)^{-1} \tag{2.9}$$

The important point for this method is that the number of measurement sets in k directions should be greater than the number of the elements N to avoid the matrix singularity problem in the resulting matrix of $(A_k A_k^H)$. If the number of unknowns is less than number of equations, system will be overdetermined and an exact or an approximate solution set can be found.

Another important point with the use of this method is that structure scattering cannot be modeled easily with few parameters. On the other hand, for a large array, since all elements are affected similarly by the structure scattering, one can find an appropriate *Z* matrix including both mutual coupling and structure scattering effects.

2.3.7 CALIBRATION METHOD USING MUTUAL COUPLING IN BEAM FORMING NETWORK

Calibration method using mutual coupling in beam forming network relies on the signal variation of the beam forming network (BFN) output due to rotation of the excitation phase [24]. This method aims to calibrate transmission lines but not directly coupling between antenna elements.

The advantage of this method is that the package structure of beam forming network, or equivalently integration of BFN, is not decomposed. Any external antenna or probe is not used. Relevant measurements are taken with the help of a Network Analyzer.

The amount of coupling in the BFN is dependent on the structural configuration such as transmission lines spacing, substrate material, arrangement of electrical components, and package dimensions of the BFN. Therefore, compensation of coupling is based on experimental evaluations rather than numerical calculations and analysis.

Calibration procedure is very similar to the REV method; the only difference is that while the REV method measures the electric field by free space propagation from the antenna elements, this method measures the electromagnetic waves propagating along the transmission lines. The procedure involves rotating the phase states of elements and normalization of vector variances according to initial state value of each port in order to compute the coupling compensation coefficients.

Figure 7 shows a block diagram of the calibration configuration. The network analyzer is connected to the output of the tested element instead of radiator.

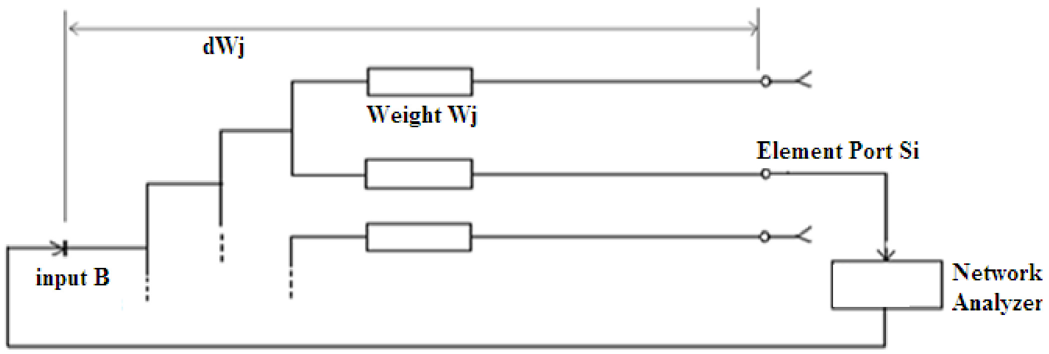

Figure 7. Configuration for the mutual coupling based BFN calibration using a Network Analyzer.

In **Figure 7**, B is the input signal to the BFN which is injected by network analyzer to the system, dW_j denotes the fixed change in the amplitude and phase along the path, and W_j the weighting of the j^{th} element. Received signal from the i^{th} element port is,

$$S_i = B \sum_j C'_{ij} \; dW_j \; W_j = B \sum_j C_{ij} \, W_j \tag{2.10}$$

where $C'_{ij} \, dW_j = C_{ij}$. The aim is to find C matrix, which is in turn used to obtain calibrated weight matrix via the formula,

$$[W_j^c] = [C_{ij}][W_j] \quad (2.11)$$

where $[W_j]$ is the desired excitation weight.

As depicted in **Figure 8**, rotating the phase of the j[th] branch results in the signal output at port i to vary in a sinusoidal fashion. The coupling coefficient s_{ij} is derived from relevant sinusoid's maximum and minimum values, and phase step value for the maximum point of this sinusoid. Finally, C_{ij} values can be extracted with the formula,

$$C_{ij} = (s_{ij}S_{i0})/(W_{j0}B) \quad (2.12)$$

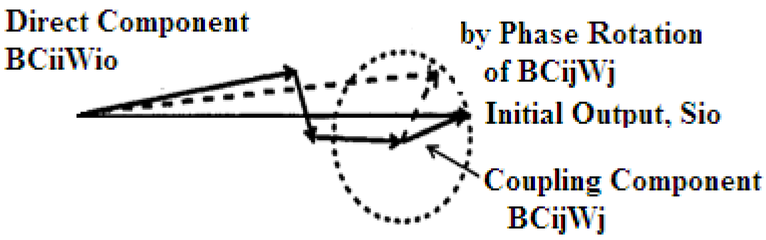

Figure 8. Combined vector position due to coupling vector rotation cited in [24].

2.3.8 MUTUAL COUPLING COMPARATION-BASED CALIBRATION METHOD OF PHASED ARRAY ANTENNAS

Mutual Coupling Comparation-Based Calibration Method basically uses the inherent mutual coupling among the radiating elements. It is based on the idea that mutual coupling is the same for all like pairs of adjacent elements in the array aperture.

Figure 9 shows a sample configuration of antenna array aperture. The procedure of implementation of this method can be divided in three steps. The first is the calibration of odd columns (denoted by A). Second step is calibration of even columns (denoted by X) and the last step is establishing the relation between the odd and even column elements.

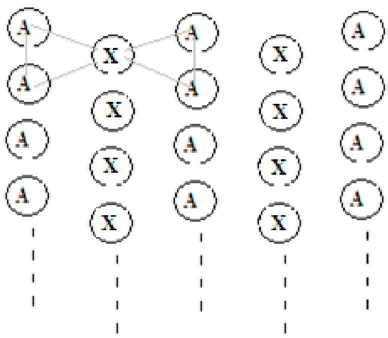

Figure 9. Calibration scheme for the mutual coupling based phased array antenna calibration.

The odd-column calibration is achieved by calibrating four A elements circulated around one X element at one time as shown in **Figure 9**. While X is transmitting, four A elements are calibrated such that they yield the same voltage output. Then, using two of the previously calibrated A elements, the next A-pair (which are elements of adjacent odd columns) is calibrated. Even-column calibration is performed in a similar way by merely exchanging the roles of A and X elements. For the third step, the paper [27] states a way of setting the relation between odd and even columns. The cited way is that an A element in the odd column will transmit and signals received from the nearest X element and the nearest A element will be measured. Subsequently, an X element will transmit and signals received from the nearest X element and the nearest A element will be measured. Then, the ratio of each measured value is calculated and with the cross-multiplication of these, the complex ratio *t* which ties odd and even columns is calculated.

In [27], a design hint which suggests that there should be at least two rows of dummy elements around the aperture periphery for low-sidelobe and low RCS designs is given. The proposed method can be achieved both for isosceles triangle grids and for equilateral triangle grids.

Another similar calibration procedure is stated in [30] which also uses of mutual coupling between array elements. According to the mentioned invention, firstly, an element is selected for calibration. Then, the power to be delivered to this element is determined according to a consideration of linear dynamic range of nearby elements and SNR requirements of far elements. In **Figure 10,** the outer circle P marks the SNR boundary and elements in the outside of the inner circle S are receiving elements in their linear dynamic ranges while TE is transmitting. The RA region (annulus inside of P circle and outside of S circle) is the calibration area.

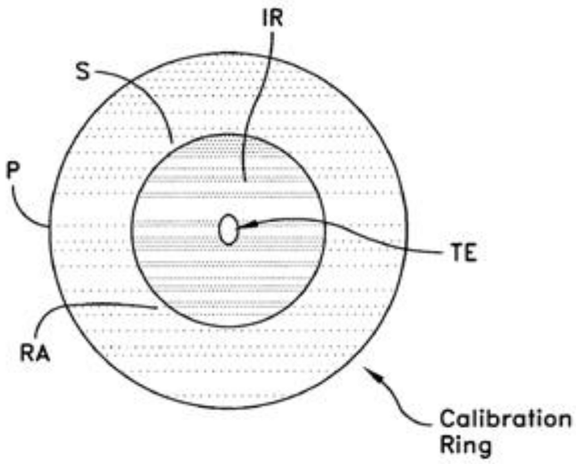

Figure 10. Calibration circle in the alternative mutual coupling based method in [30].

This latter method of calibration can be realized in two modes: The transmit mode of operation and the receive mode of operation. As expected, the mode type depends on the operation mode of element under test to calibrate. For transmit mode of calibration, a test element is chosen, define as A, then its calibration circle is drawn and a second element (call B) is selected. After that, a reference element C is selected which is in the calibration ring of the element B and symmetric to A about B.

Aforementioned configuration is illustrated in **Figure 11**. The elements A and C both transmit a signal and element B receives via the inherent mutual coupling. Then, phase shifter of element A is adjusted to see a null and after finding the null, attenuator of A is adjusted to observe the sharpest null. Determined phase shifter and attenuator states are subsequently recorded and are treated as calibration coefficients. Relevant procedure is repeated for a range of frequencies.

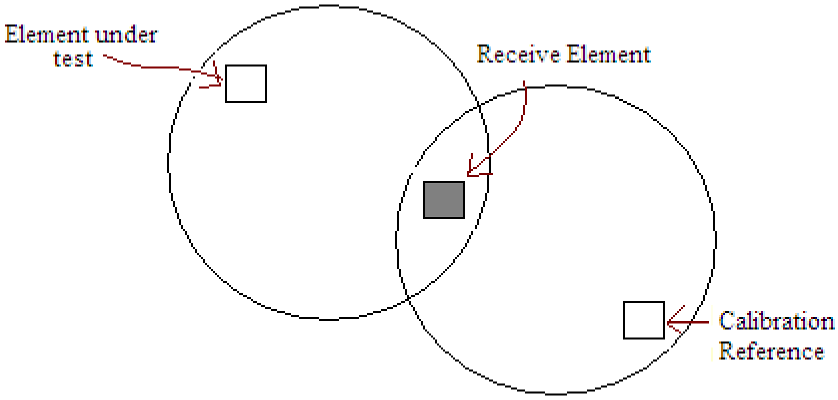

Figure 11. Configuration for the alternative mutual coupling based method.

The receive mode of calibration procedure is essentially the same as the transmit mode except that the element B transmits while A and C receive. Again, phase shifter and attenuator of the tested element are adjusted to detect the optimum null.

2.3.9 ADDITIONAL COUPLERS-BASED CALIBRATION METHOD

Additional Couplers-Based Calibration Method is from the reference [31] and it uses additional couplers for calibration of an array. The elements having directional coupler ports in their paths are named as kernel elements. The general structure of calibration method is shown in **Figure 12.**

The basic approach for the mentioned calibration is that signals are applied to the beamformer port feeding the kernel element and then, the beamformer path to the kernel element is determined by knowing directional coupler port length to the additional calibration unit (shown as $D_{i,j}$). The non-kernel elements near the kernel are calibrated with the signal coming from the beamformer to the non-kernel element and by receiving this signal through a calibration path of the kernel element by the help of mutual coupling.

First, the directional coupler paths should be characterized. If the signal is applied from $\mathrm{D}_{1,1}$ and received by $\mathrm{D}_{1,2}$, this path contains $\mathrm{L}_{1,2}$ which stands for the electrical length through the directional coupler from port 1 to port 2. Therefore, equation $\frac{1}{2}(\mathrm{D}_{1,1} + \mathrm{D}_{1,2} - \mathrm{L}_{1,2})$ will give the one calibration path.

After characterizing the calibration paths, the signal is applied from beamformer input and received by calibration unit through port 4 to 2 and then $\mathrm{D}_{1,2}$. Since the calibration path between port 2 and $\mathrm{D}_{1,2}$, and electrical length through port 4 to 2 are known; the beamformer path plus T/R module can be derived. According to procedure of the invention, these values are compared to a set of stored information in control computer. If they are same, this step is completed; if they are not same, values are updated and this step is completed.

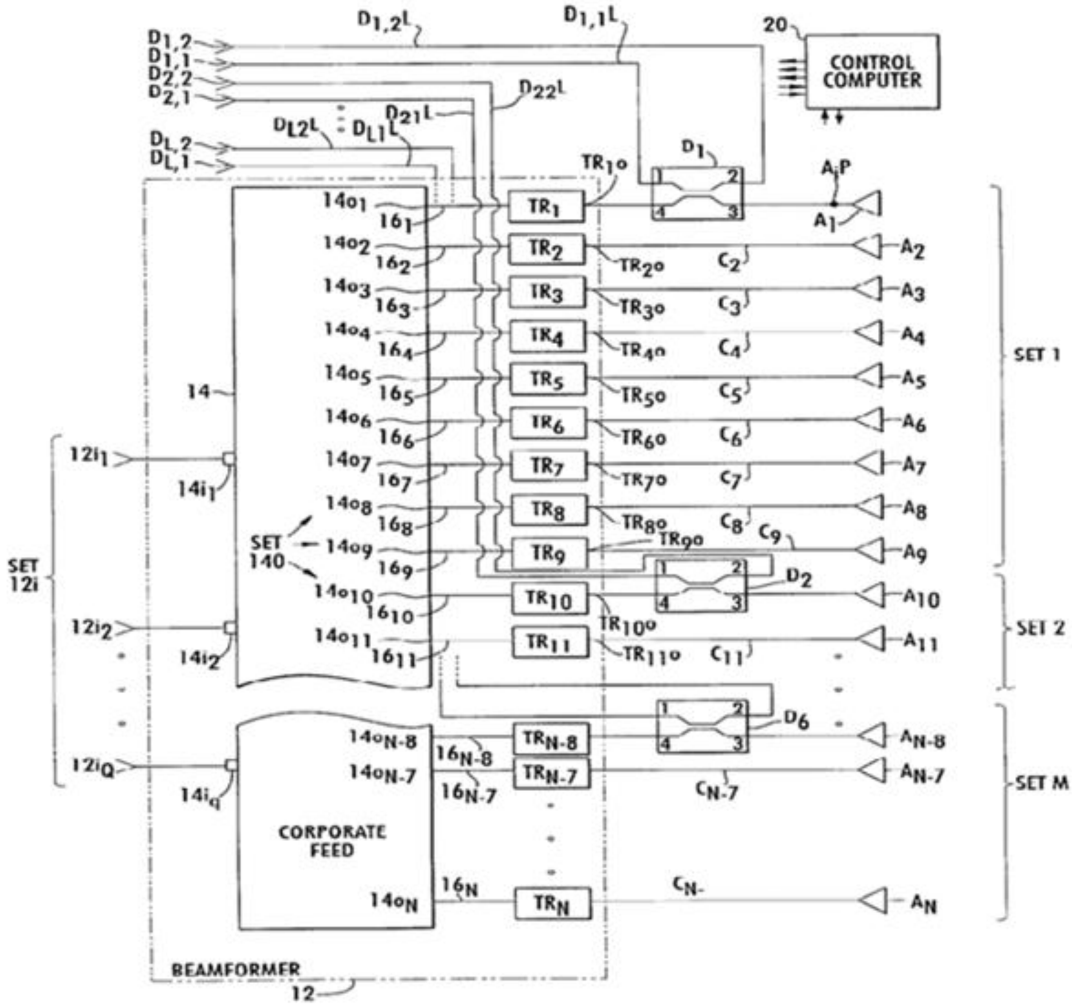

Figure 12. Block diagram for the method of [31].

After calibrating kernel elements, the non-kernel elements near kernel should be calibrated. To decrease number of kernel elements and so the number of directional couplers, an example configuration is shown in **Figure 13**.

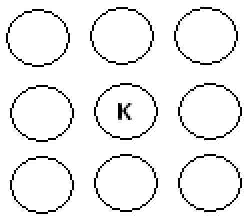

Figure 13. Kernel element location.

The procedure for non-kernel element characterization is as follows: use radiation part of the kernel path and the signal is applied from calibration unit through directional coupler port 1 to port 3. Then, selected non-kernel element receives the signal via mutual coupling and corresponding value is measured from the network output. This measured value contains $D_{1,1L}$, therefore $D_{1,1L}$ is subtracted from this value and the procedure again continues with the comparison between measured and previously stored data.

2.4 GENERAL ASSESSMENT OF LITERATURE SURVEY

The chapter of literature survey is ended by explaining nine of the existing calibration methods for Phased Array Radars. These methods include both internal measurement based methods such as using mutual coupling via directional couplers and external measurement based methods such as REV and MEP methods.

REV and MEP methods are explained in detail in the following chapters. The main reason behind focusing on REV and MEP methods is aiming to see overall error in the radiation without any need to change the system set up. The REV and MEP method do not need internally added active or passive components which extend the system budget in terms of cost and complexity.

The MEP method is a fast calibration method since elements are simultaneously measured and calibrated. On the other hand, it should be noted that there is a tradeoff between time consumption and accuracy. The MEP method will be faster but in that case, the accuracy will worsen. The step size of the phase rotation of individual element in REV and MEP methods determines required time for calibration and the time consumption is adjustable in exchange for accuracy according to the application.

The use of external antenna causes the main disadvantage of REV and MEP methods. The probe antenna is located at a certain distance from the array and since in situ calibration is performed in the operation environment, measurements are exposed to influences such as multipath effects, scatterers, interference, weather conditions. These environmental influences affect the accuracy of the calibration and enhance required time for observing array radiation characteristic due to random changes.

The examinations on REV and MEP methods will be expanded with giving simulations and detailed procedures of aforementioned methods in the following chapter.

CHAPTER 3

EMPHASIS ON MEP AND REV METHODS

Chapter 2 elaborated a diverse selection of phased array calibration methods existing in the literature. At the end of this extensive literature survey, MEP and REV methods are noted to draw more attention than other methods due to their favorable qualities such as their systematic nature, ease of applicability, and less demanding hardware requirements. Consequently, subsequent research focuses on these latter methods and MEP and REV methods are evaluated in many aspects, using simulations. In the following sections, simulation results are presented.

In order to demonstrate successful operation of the selected calibration methods, performance of each method has been evaluated in MATLAB® simulation environment using several configurations serving as test vehicles. In the subsequent subsections, these test configurations are described for each calibration method and obtained simulation results are given.

3.1 MEP METHOD AND SIMULATIONS

In **Figure 14**, implementation procedure of MEP method is stated step by step. Information about phase increments and simulations to explain implementation of MEP method to sample arrays are presented in this section.

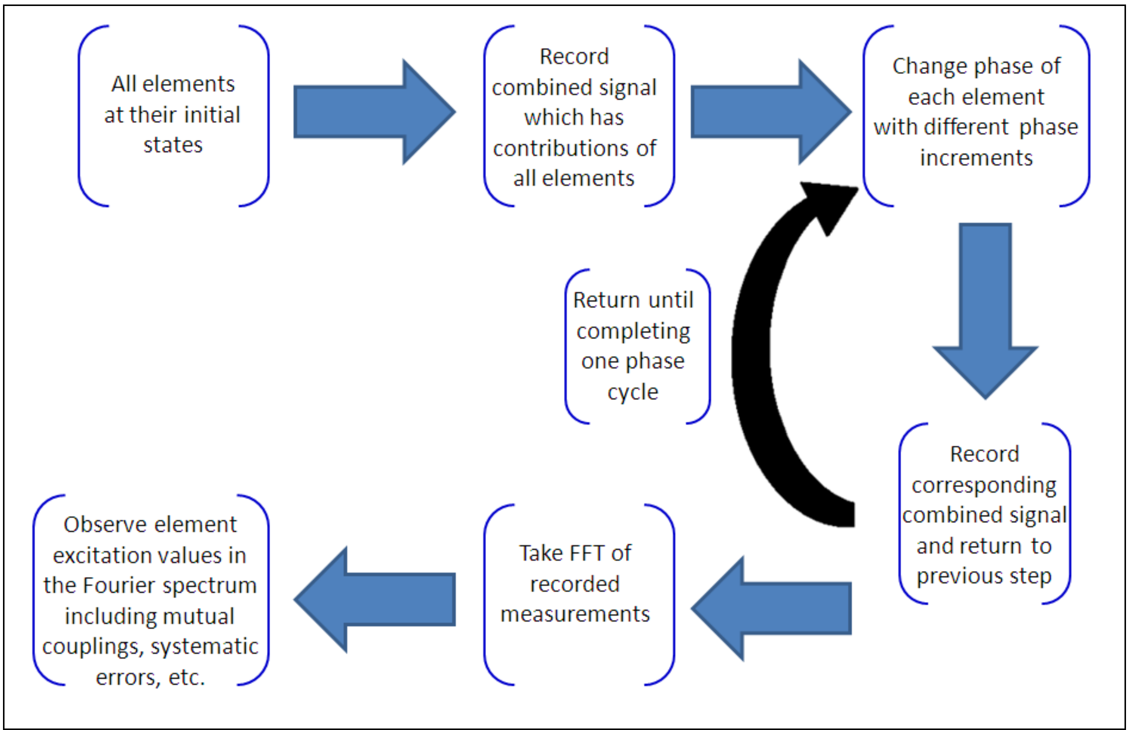

Figure 14. Step by step implementation procedure of MEP method

Before explaining the MEP calibration on a sample array, determination of phase steps should be stated. Firstly, the phase of any element in the calibration subset is rotated with sequential (identical increments) phase steps around 360° to keep periodicity which yields the use of Fourier approach. One cycle of phase rotation has to be completed for every element. Widths of phase step intervals are different for different elements to make weighting coefficient of different elements fall in different bins of Fourier spectrum.

Another point about the procedure of MEP is the choice of the number of phase levels, in other words, determining how many bit phase shifter is needed to calibrate group of elements. The number of phase levels is directly related with the number of elements which will be simultaneously calibrated. In [1], it is claimed that elements whose count is half of the number of phase levels can be calibrated at the same time.

A sample linear array of four elements can be relevant to exactly state the procedure of the method. For this array at least 3-bit phase shifter should be used.

Measurements are made by changing phase state of first element one by one which corresponds to 45° phase increments, the second three by three corresponding to 135° increment, the third five by five corresponding to 225° increment and the forth seven by seven corresponding to 315° phase increment. After taking the signals with eight measurements which provides one cycle in phase of each element, FFT transform of measured signals are taken. As a result, the weighting coefficients are acquired for these four elements in Fourier spectrum according to their phase change steps. The point zero at Fourier spectrum corresponds to fixed component which is the contribution of environment (including elements which are not rotated for a large array during calibration).

In the simulation, it is assumed that the external antenna which is essential to implement the MEP method is along the array boresight direction and located in the far field of the array. Therefore, the simulation is performed according to the far field conditions. These conditions require that incident wave to the array aperture is in the plane wave form. Since the external antenna is also in the boresight of the array, there is no need to consider additional phase terms due to interelement spacings. Moreover, the far field condition removes the necessity of using additional magnitude coefficients for each element of the array.

A 4 by 4 planar array with half wavelength spacing is simulated in the MATLAB® with the following complex excitation coefficients which are shown in **Table 1**:

Table 1. Excitation coefficients of the sample array in simulation

E_1=4.0+1.0j	E_2=3.5	E_3=3.0	E_4=2.5
E_5=2.0	E_6=1.5	E_7=1.0	E_8=1.0
E_9=3.5	E_{10}=3.0	E_{11}=2.5	E_{12}=2.0
E_{13}=1.5	E_{14}=1.0	E_{15}=4.0	E_{16}=3.0+1.0j

Excitation coefficients computed by the MEP method for the ideal case is given in **Figure 15** and **Figure 16** for the real and imaginary parts respectively. It is observed from these plots that actual excitation coefficients are successfully extracted for this array configuration.

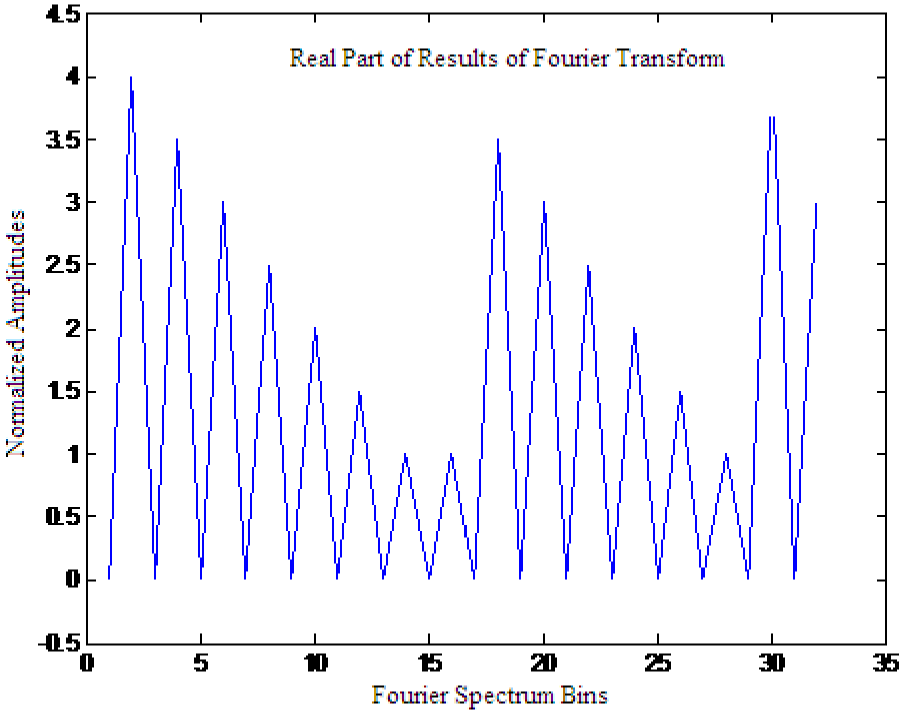

Figure 15. Real part of 16 element array excitation coefficients determined with the MEP method.

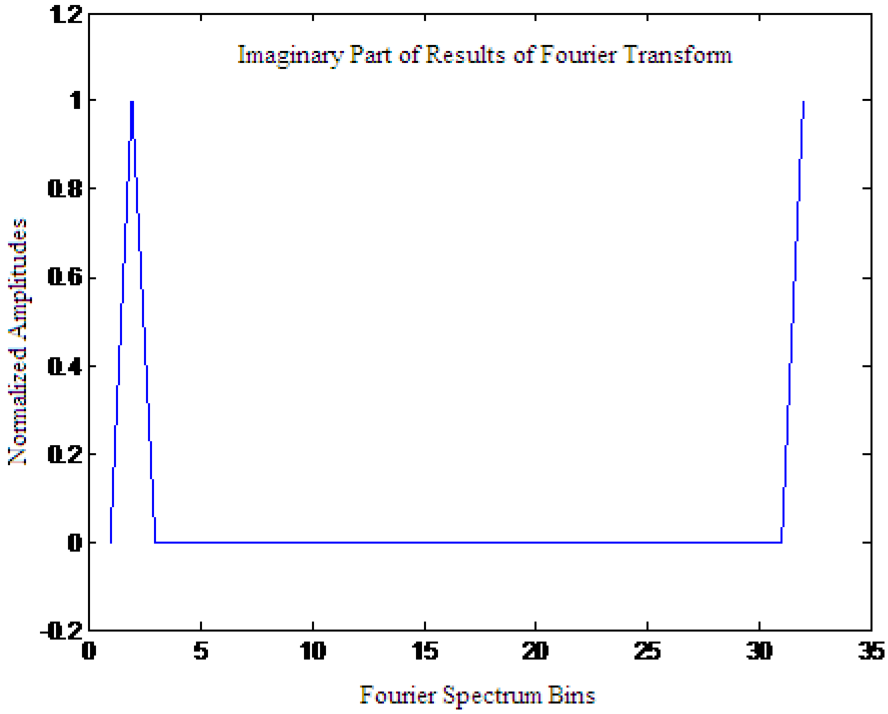

Figure 16. Imaginary part of 16 element array excitation coefficients determined with the MEP method.

In simulation experiments, it is seen that the number of elements to calibrate simultaneously can increase up to (N-1) elements where N is the number of phase levels.

The reason behind this maximum number, (N-1), is the possible existence of direct component from environment or the radiating system itself. In the case of implementing the procedure to N elements simultaneously, the direct component and the element having largest phase step will be superposed and appear in the first bin of the Fourier spectrum. In other words, calibration of M number of elements requires at least (M+1) measurements and so (M+1) phase levels. Simulation with respect to values of elements in **Table 1** is also performed by using smaller phase steps to show number of elements to be calibrated simultaneously can be increased with the use of same phase shifter and result is shown in **Figure 17**.

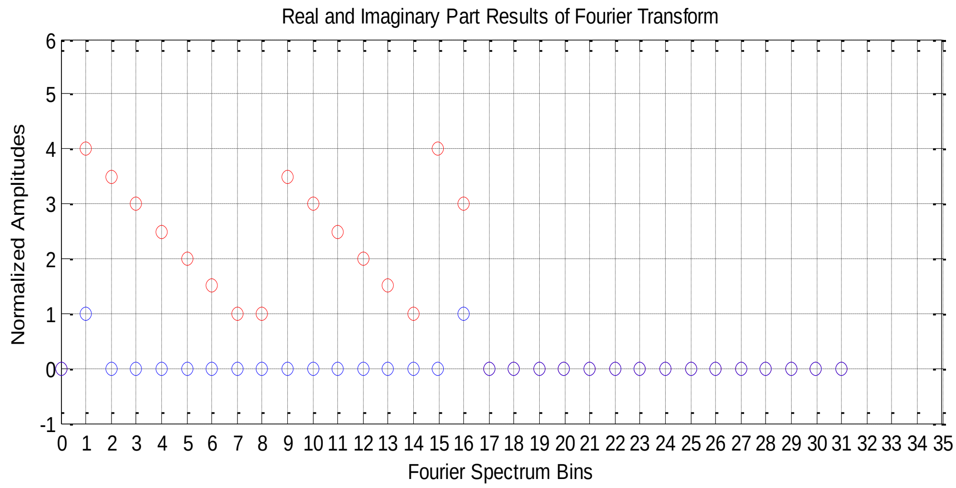

Figure 17. Real and imaginary part results of Fourier Transform **(**red circles and blue circles represent real and imaginary normalized values of elements respectively.)

As a different configuration, a planar array of 15 (3 by 5) elements is also simulated to show the use of the method for rectangular arrangement. The excitation coefficients, which are taken as real, for this latter case are shown in **Table 2:**

Table 2. Excitation Coefficients for 15 (3 by 5) elements array

E_1=4	E_2=3.5	E_3=3	E_4=2.5	E_5=2
E_6=1.5	E_7=1	E_8=1	E_9=3.5	E_{10}=3
E_{11}=2.5	E_{12}=2	E_{13}=1.5	E_{14}=1	E_{15}=4

Excitation coefficients determined by the MEP method for the ideal case is given in **Figure 18**, which again shows excellent agreement between the actual and extracted values.

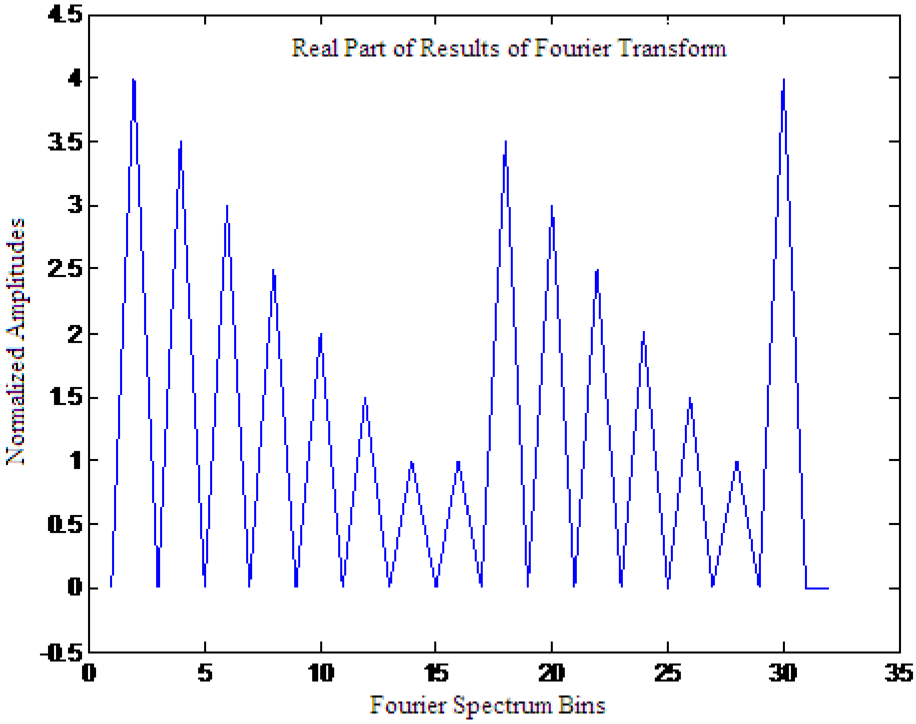

Figure 18. 15 element array excitation coefficients after MEP method (real-part).

In order to give more insight about the operation principle of the MEP method, this method is simulated in 3-D for a 4 by 8 phased array to simulate experimental set-up which will be explained in detail in the next chapter. This array contains 8 subarrays and each subarray contains 4 elements in vertical arrangement. Four elements in one subarray are excited by single mutual vector modulator. By simulating this antenna array, experimental results presented in the following sections could be thoroughly interpreted. The phased array configuration in the simulations represents the actual antenna array system which will be explained in Chapter 4. Previously measured active element patterns are used in the simulation. Assuming correct phase settings, the expected measurement results are obtained by using MATLAB® based on analytically derived equations.

MEP method itself, in essence, corresponds to beam steering action of the antenna pattern and individual measurements at different phase settings is equivalent to the sampling of the array pattern scanned to different angles. For every set of phase values applied to the eight 4 by 1 sub-arrays, pattern will steer ideally as shown in **Figure 19.(a)** through **(h)**. Required phase values for each step of this simulation are listed in **Table 3**.

Table 3. Phase values (in degrees) of elements for the simulated 16 signals.

	ELEMENTS							
	1st	2nd	3rd	4th	5th	6th	7th	8th
Step-1	0	0	0	0	0	0	0	0
Step-2	22.5	67.5	112.5	157.5	202.5	247.5	292.5	337.5
Step-3	45	135	225	315	45	135	225	315
Step-4	67.5	202.5	337.5	112.5	247.5	22.5	157.5	292.5
Step-5	90	270	90	270	90	270	90	270
Step-6	112.5	337.5	202.5	67.5	292.5	157.5	22.5	247.5
Step-7	135	45	315	225	135	45	315	225
Step-8	157.5	112.5	67.5	22.5	337.5	292.5	247.5	202.5
Step-9	180	180	180	180	180	180	180	180
Step-10	202.5	247.5	292.5	337.5	22.5	67.5	112.5	157.5
Step-11	225	315	45	135	225	315	45	135
Step-12	247.5	22.5	157.5	292.5	67.5	202.5	337.5	112.5
Step-13	270	90	270	90	270	90	270	90
Step-14	292.5	157.5	22.5	247.5	112.5	337.5	202.5	67.5
Step-15	315	225	135	45	315	225	135	45
Step-16	337.5	292.5	247.5	202.5	157.5	112.5	67.5	22.5

As can be seen in **Table 3**, phase values while taking second combined signal in step-2 are 22.5°, 67.5°, 112.5°, 157.5°, 202.5°, 247.5°, 292.5°, 337.5° and the other steps contain multiples of step-2. If phase values in step-2 are taken with 22.5° phase increments and the other steps are taken as multiples of these values, the number of elements which can be calibrated at the same time increases up to 15 by this new phase excitation procedure which has a similar form explained in **Figure 17**.

Using odd multiplies of increments in phase rotation of elements while taking each combined signal aims to separate values of contiguous two elements by inserting a deep between these two values.

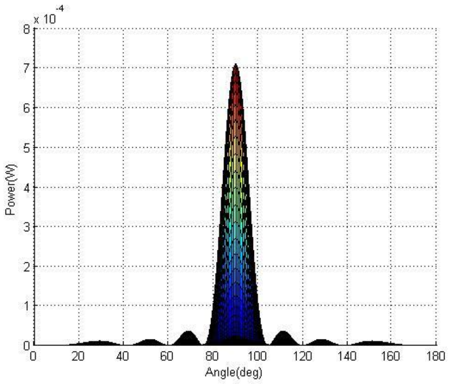

(a) 0th MEP state.

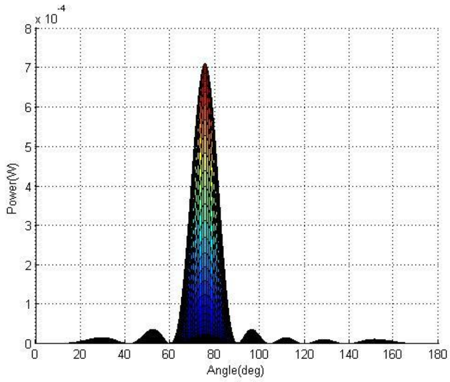

(b) 1st MEP state.

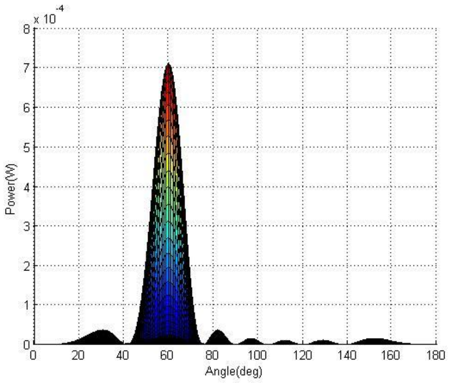

(c) 2nd MEP state.

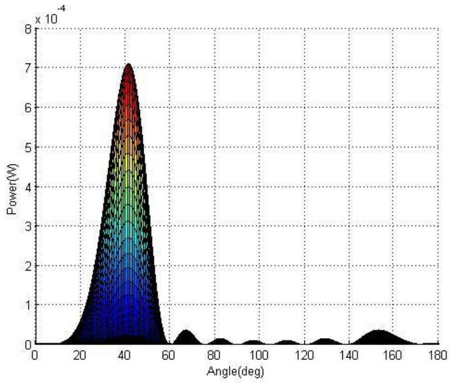

(d) 3rd MEP state.

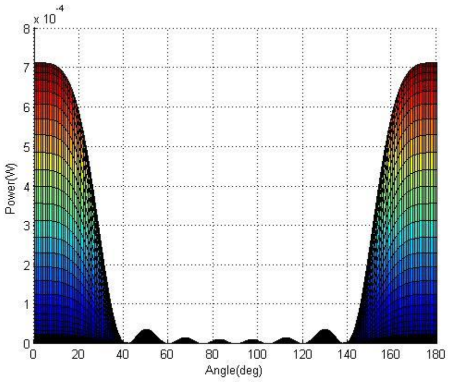

(e) 4th MEP state.

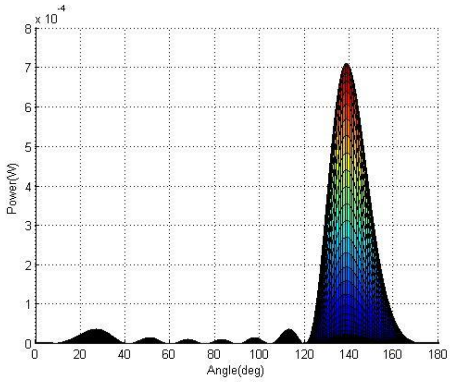

(f) 5th MEP state.

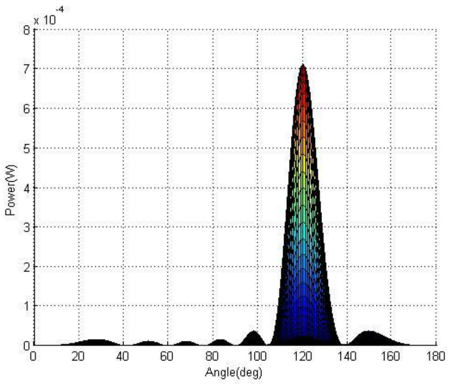

(g) 6th MEP state.

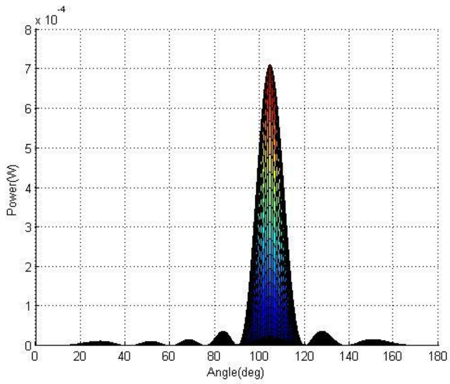

(h) 7th MEP state.

Figure 19. Beam steering and sampling action of the MEP method illustrated for the 4 by 8 phased

array. Subarrays are aligned along the Z-axis in simulation.

In **Figure 19.(a)-(h),** simulations results for the first eight steps out of 16 are provided since remaining steps are mere repetitions of the first 8 steps. The result of the simulation for uniform excitation coefficients is shown in **Figure 20**. It can be seen that eight excitation values are close to the expectations (red-line) but not exactly the same; an observation which reflects the non-identical active element patterns.

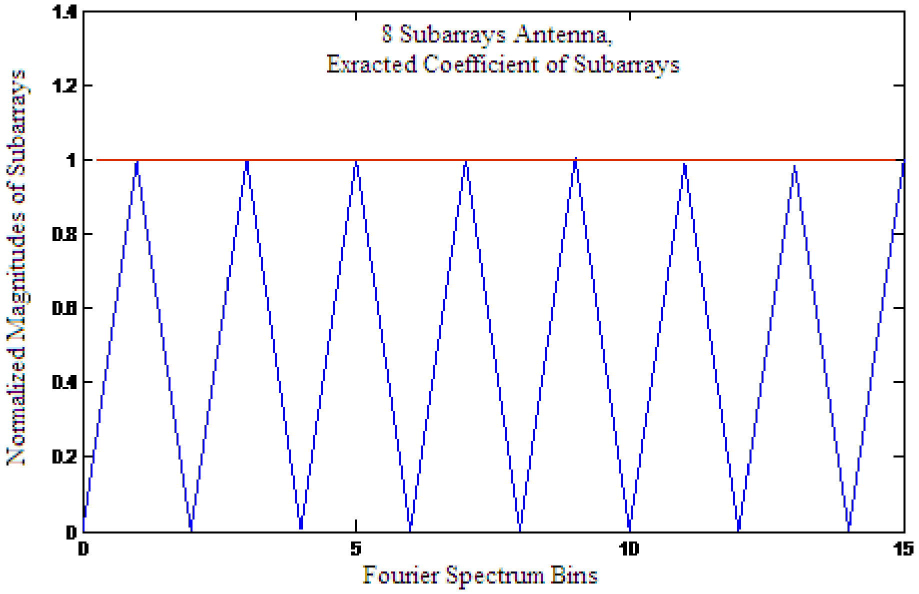

Figure 20. Extracted normalized excitation coefficients with respect to the 8th element using the MEP method.

According to the implementation results of this method, constraints and limitations of this method can be mentioned as;

Firstly, the external antenna should be located in the boresight of the array (it should be on rotation center of the array), position error in the placement of the external antenna will give erroneous results due to occurrence phase differences between array elements.

Secondly, it is stated that the number of elements to be calibrated should be equal or less than half of the number of phase states of phase-shifter or vector modulator part, however; the number of elements to be calibrated simultaneously can be equal to the number of phase states minus one by exciting elements with proper phase values.

Finally, according to results, measurements should be performed in the far field of the array, near field measurements may also work if the contributions of distance ratios are accounted for in the calculations.

In the literature, One Square Meter Array (OSMA) is an example of implementation of MEP calibration [1]. OSMA is a demonstrator receive-only active phased array antenna system for the development of very sensitive radio telescope Square Kilometer Array (SKA) [2]. In **Figure 21**, MEP method implementation to an array of 8 by 4 elements is shown to get phase offset errors of elements. There are eight subarrays each of which contains four elements. Each elements in the subarray has phase shifter and attenuator.

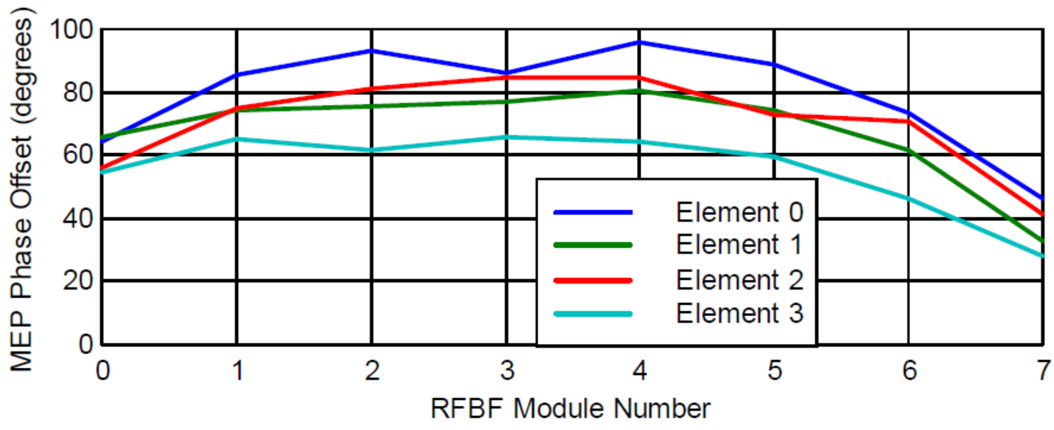

(a)

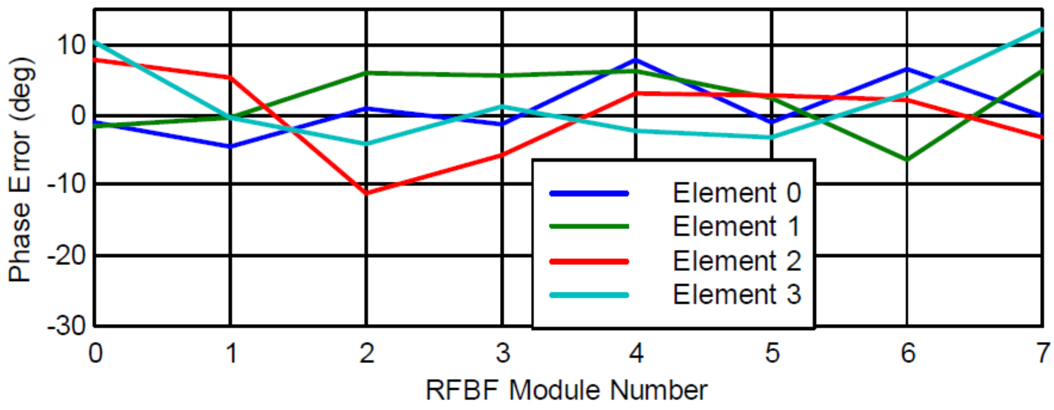

(b)

Figure 21. Extracted phase off-sets with MEP (a) and phase errors after calibration (b) from [1].

In **Figure 21**, each module number of RF beamformer unit (RFBF) corresponds to one subarray. As it is seen in **Figure 21.a**, phase offsets are in a range from 30° to 100° and these phase offset values are in a range from -10° to 10° in part b after corrections.

MEP method can be applied to large scale arrays by grouping elements and rotate their phase states with the same increments. This approach is very similar to the approach used in CREV method. By grouping elements, array can be divided into blocks and blocks are treated as individual elements.

Observing limitations and requirements of MEP method, it can be applied to phased arrays with reliable phase shifters easily.

3.2 *REV METHOD AND SIMULATIONS*

In the REV method, the probe is located in the far field of the array element; which may be in the near field of the array. The probe antenna distance from the array should not be too much in order to avoid unwanted effects of the electromagnetic environment in the test field on measurement accuracy.

An important point about the REV method is that measured value by the pick-up antenna used in the REV method contains the mutual coupling effects among antenna elements, variation of antenna element characteristics due to environmental conditions, placement error of antenna elements, effects of scattering from nearby obstacles, imperfectness of the feed system, etc.

The only electrical length deviation of the feed system and mutual coupling between antenna elements (if single mode excitation is implemented) are independent from observation direction of the REV measurement. All other effects depend on angle.

As it is illustrated in **Figure 22,** REV procedure starts with all elements at their initial phase states. Then, the phase state of the tested element is rotated and combined signals which consist of other elements and tested element contribution vectors are measured. After that, set the tested element phase state to its initial state, and go to the adjacent element to get its measurement set with rotating its phase state. By doing so, measured maximum and minimum signal levels gives information about the phase and the magnitude of the each tested element. In the case of using analog phase shifter, the phase shift value which makes contribution of rest elements and tested element co-phase can be seen clearly since it will give a maximum.

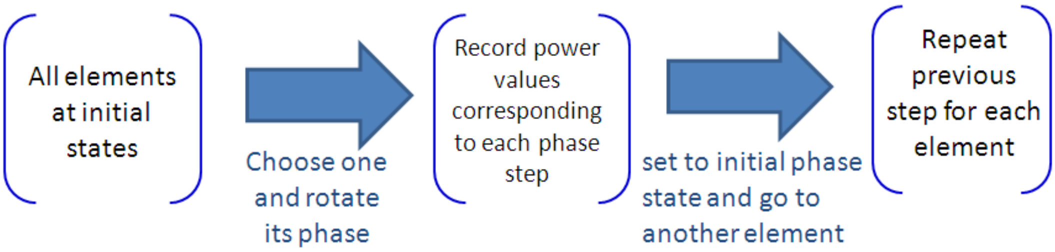

Figure 22. Block diagram to be followed while taking REV measurements

In the case of using digital phase shifter which gives discrete phase shifts, acquiring exact phase shift can be a problem due to discrete values; however, the paper [17] provides an analytic solution way from which combined vector components can be calculated from approximate formulates.

According to [17], non-rotating component of combined signal is denoted by $A_1 exp(j\phi_1)$ and rotating component $A_2 exp(j\phi_2)$, Δ is the additional phase of $A_2 exp(j\phi_2)$ contributed by the phase-shifter and equal to the multiplication of phase state number i and phase step interval δ. After combined signals $A(i)$ are measured for each phase state of tested (rotated) element, rotating electric field and non-rotating electric field can be calculated with formulas from (3.1) to (3.5),

$$I = \sum_{i=0}^{M-1} A^2(i)\cos(i\delta) \qquad Q = \sum_{i=0}^{M-1} A^2(i)\sin(i\delta) \tag{3.1}$$

$$A_1^2 + A_2^2 = \frac{1}{M}\sum_{i=0}^{M-1} A^2(i) \tag{3.2}$$

$$A_1 A_2 = \frac{1}{M}(I^2 + Q^2)^{1/2} \tag{3.3}$$

$$A_1^2 + A_2^2 = C \qquad A_1 A_2 = D \tag{3.4}$$

$$\begin{aligned} A_1 &= (\sqrt{C+2D} + \sqrt{C-2D})/2 \\ A_2 &= (\sqrt{C+2D} - \sqrt{C-2D})/2 \\ \phi_2 - \phi_1 &= \arg(I - jQ) \end{aligned} \tag{3.5}$$

Equations in (3.5) give magnitudes of rotating and non-rotating electric fields which form measured combined signals and initial phase difference between rotating and non-rotating electric field vectors. As it can be seen from equations, only magnitudes of measured signals are used as input and there is not any necessity of phase information for the REV process. Moreover, phase information for the tested element can be extracted with respect to the non-rotating reference signal.

A similar method to the REV takes place in the literature with the name as MTE in the paper [13]. The MTE method which is used to compare initial amplitude and phase states of each element differs from the REV method. by such a condition of implementation procedure that other elements are turned off while tested element is rotating. Moreover, in the MTE method, the phase rotation of the tested element is performed, but in this case, combined signal consists of only the reference signal vector from an external or internal fixed source and the tested channel contribution vector. The use of reference signal vector gives relations between all channels amplitude and phase states with respect to the reference.

In the experiments, turning-off other elements does not seem to be a good idea to implement, since load conditions, and so coupling coefficients, will change whether other elements are turned-off or turned-on. Therefore, experiments which are tried to perform MEP method take other elements as the reference element and algorithms intended for the solution of MEP method with respect to use of this type of reference are redesigned which will be explained in detail in Chapter 4.

Similar to the MEP method, simulations for the REV method are also conducted in MATLAB® environment. Firstly, an array consisting of four elements is simulated with phase steps of 45°. In particular, element excitations are taken as in **Table 4**:

Table 4. Excitations of sample 4 element array

Ex(1)	Ex(2)	Ex(3)	Ex(4)
3.0	2.0+2.0j	3.0	2.0-2.0j

and reference component is taken as 5.0.

Simulated power variation due to phase rotations of elements is shown in **Figure 23.(a)** to **(d)** for each rotated antenna element.

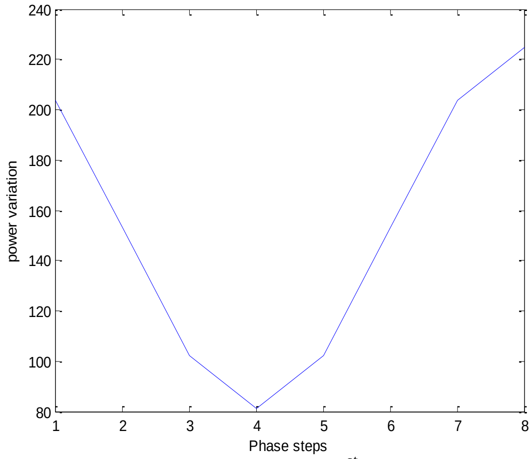

(a) Phase rotation of the 1st element.

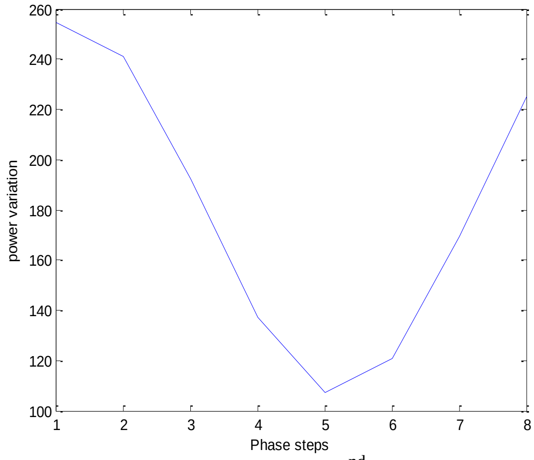

(b) Phase rotation of the 2nd element.

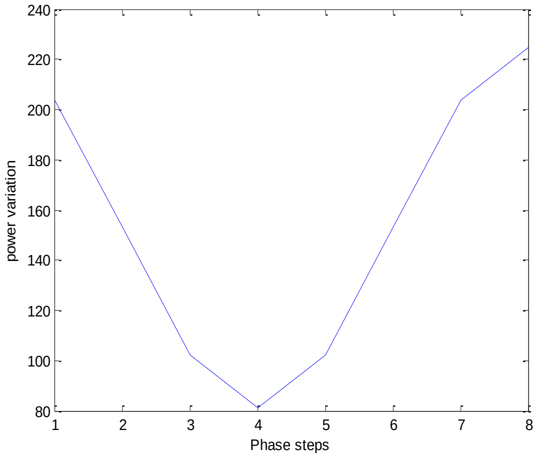

(c) Phase rotation of the 3rd element.

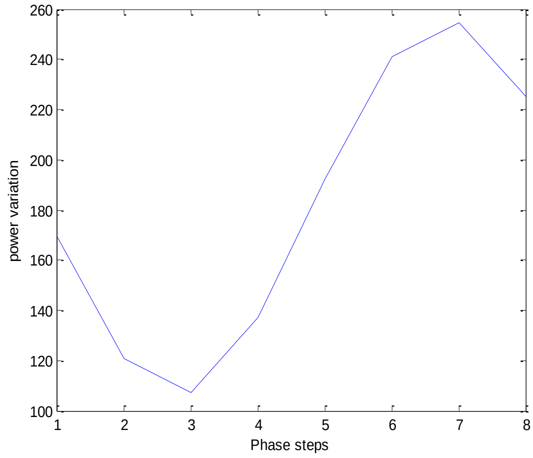

(d) Phase rotation of the 4th element.

Figure 23. Power variation due to individual phase rotation of element excitations with 45° steps.

Excitation coefficients of the four elements are extracted by MATLAB® as in **Table 5**,

Table 5. REV simulation results for used 3-bit digital phase shifter

Ex(1)	Ex(2)	Ex(3)	Ex(4)
3.0000	1.6726 +2.2809j	3.0000	1.6726 - 2.2809j

Values of the first and the third elements are correct, however; the second and the fourth elements (which have phase differences from the reference element) are not. There is a difference between the actual and the simulated results. It should be noted that erroneous results have phase errors but they are correct in magnitude.

If the reference signal gets larger, phase error in extracted weighting coefficients will be smaller. While the reference element is 15, excitation coefficients of the four elements are extracted by MATLAB® as in **Table 6**,

Table 6. REV simulation results for larger reference

Ex(1)	Ex(2)	Ex(3)	Ex(4)
3.0000	1.8192 +2.1657i	3.0000	1.8192 -2.1657i

As it can be seen from two different results which correspond to two different reference signal values, the resultant error is due to the addition of the other three elements' contributions to the reference component while one element is rotating.

As a constraint of this method, the combined vector should be sufficiently large when it is compared with the tested channel contribution vector to see the variations with phase state steps.

In fact, two solutions are developed to alleviate this kind of error in the simulation development process. One remedy is to turn off other three elements while one is rotating. Second remedy is the use of iterations. In the second way, wrong MATLAB® result is taken as the element excitation value and the MATLAB® code is run again by adding values of three elements to the reference element. New values are assumed as the element excitation values again and MATLAB® code is re-run until desired number of iterations is attained.

Extracted excitation values for the four elements by the use of iterations are shown in **Table 7**:

Table 7. REV simulation results for iterative way

Ex(1)	Ex(2)	Ex(3)	Ex(4)
3	2+2j	3	2-2j

which reached their steady-state values at the 6^{th} iteration. Again there may be a need to fixed reference signal, but this time, the large reference signal is not very crucial. Moreover, iteration is very useful for implementing the CREV method. The rotating power in the CREV method can be much more than the classic REV method and this reason causes larger reference signal use. By the help of the iteration, implementation of the REV method can be easily performed with reference signal which can be comparable with or smaller than one individual element in magnitude. Since iterations are done in signal processing part digitally, they are performed very fast and they do not lead to any deceleration in the process of extracting weighting coefficients.

For the sake of clarity to understand advantage of using iteration, a simulation is generated for an array which consists of seven elements. There is also a fixed reference component. The reference component has different values for each separate implementation of the REV procedure. It is aimed that weighting coefficient results of the REV experiments should have maximum %1 error in general. Different reference components will show required iteration number to satisfy %1 error condition. Seven elements of the array which is simulated to see the benefit of the iterative way in reducing required reference have excitation coefficients which are shown in **Table 8**;

Table 8. Excitation values of sample array

Element1	Element2	Element3	Element4	Element5	Element6	Element7
1+j	1+j	1+j	1+j	1+j	1	2

Value of Reference element is firstly given as much smaller than the value of an individual element. In subsequent implementations, the value of reference element increases, **Table 9** shows increase in value of reference element;

Table 9. Magnitude of Reference element used in simulation

Values of Reference Elements									
1st	2nd	3rd	4th	5th	6th	7th	8th	9th	10th
0.1	0.5	1	2	5	10	15	20	25	35

Required number of iterations decreases with enlarging reference component as expected, it is shown in **Table 10**;

Table 10. Required number of iterations corresponding to each reference

Required Number of iterations									
1st	2nd	3rd	4th	5th	6th	7th	8th	9th	10th
371	74	37	18	7	3	2	1	1	1

In practice, generating large reference signals cannot be feasible. As it can be seen from result for required number of iterations, if iteration is not used, minimum value of the reference signal is 20 and this value is 10dB greater than the biggest individual element of the array. If the iteration is used in the implementation procedure of the REV method, a reference signal which has the same value with the biggest individual element can be enough to satisfy 1% error criteria in practice.

CHAPTER 4

EXPERIMENTAL PHASED ARRAY ANTENNA SYSTEM AND MEASUREMENT RESULTS FOR SELECTED METHODS

In addition to the simulation work provided in Chapter-3, several experimental studies were also conducted in order to assess the potential of each selected calibration method under practical conditions as opposed to ideal ones. For this purpose, the *Dual-Beam Phased Array Antenna System* [32] was utilized as the (receiving) phased array antenna under test, and each calibration method was evaluated experimentally by coupling the remote control capabilities of the relevant system with customized control routines. The architecture of the mentioned phased array system as well as the associated experimental setup is explained briefly in the next subsection. Obtained experimental findings for the MEP and REV methods are presented in the subsequent subsections.

REV and MEP method measurements are implemented using the experimental set-up in both indoor and outdoor. Additional absorbers are used for decreasing scatterings from nearby structures for indoor measurements.

4.1 EXPERIMENTAL SETUP

An adaptive, continuous-wave (CW) phased array (PA) receiver system is utilized as a test vehicle for the application of far-field calibration methods. Photographs and associated schematic diagrams of this phased array system are provided in **Figure 24** to **Figure 27.** The X-band receiver system is composed of 32 (8 by 4) antenna elements arranged in a linear array: Every vertical four elements form a sub-array and electronic control of those 8 sub-arrays is independent from each other. This system has two different receive paths which enables generation of two independent beams at the same or at different frequencies.

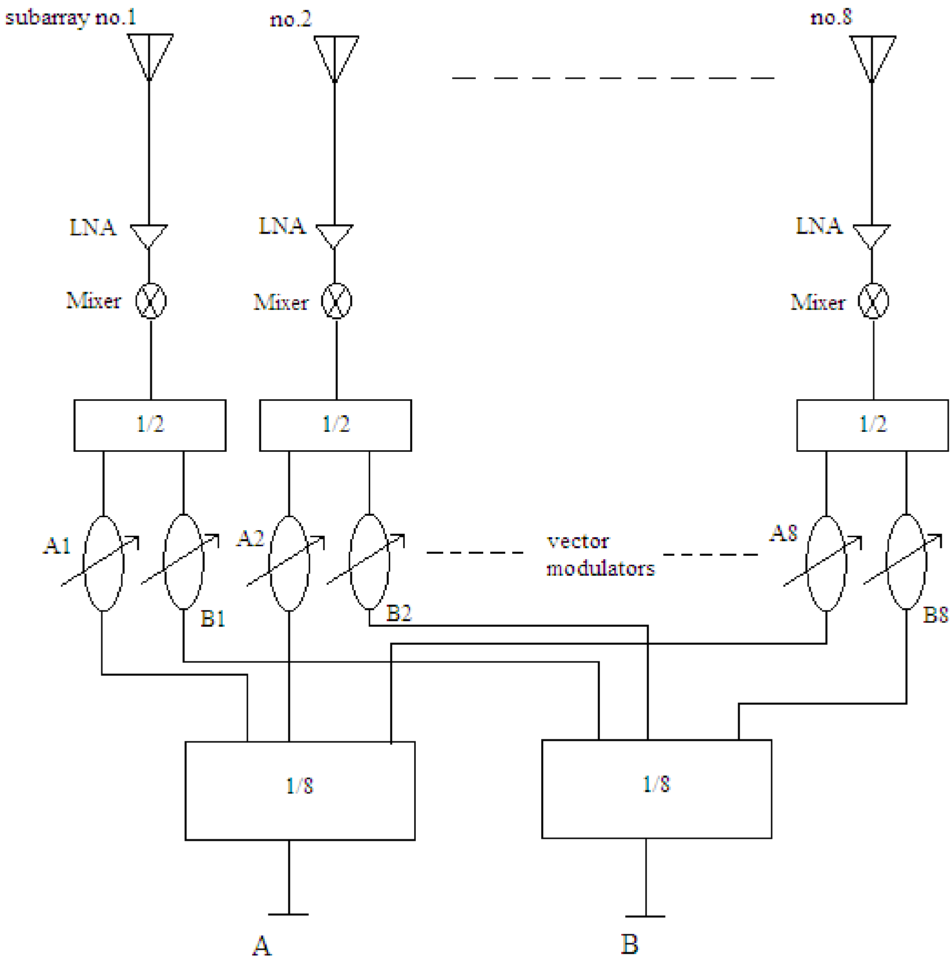

Figure 24. System block diagram of the experimental set-up.

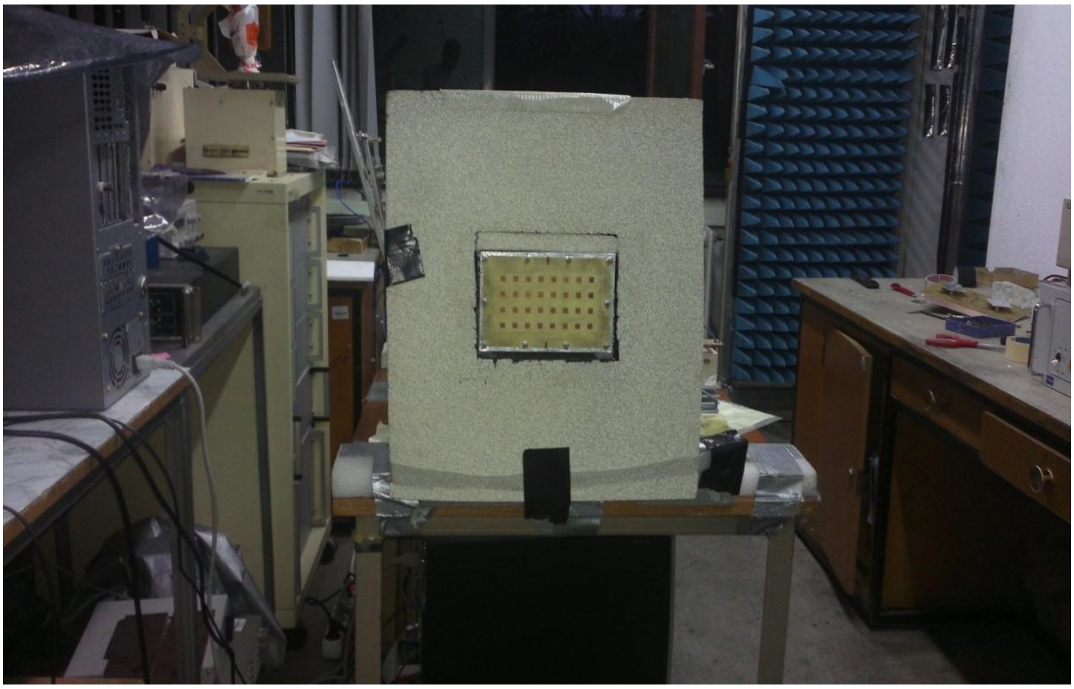

Figure 25. 4 by 8 patch antenna array (front view).

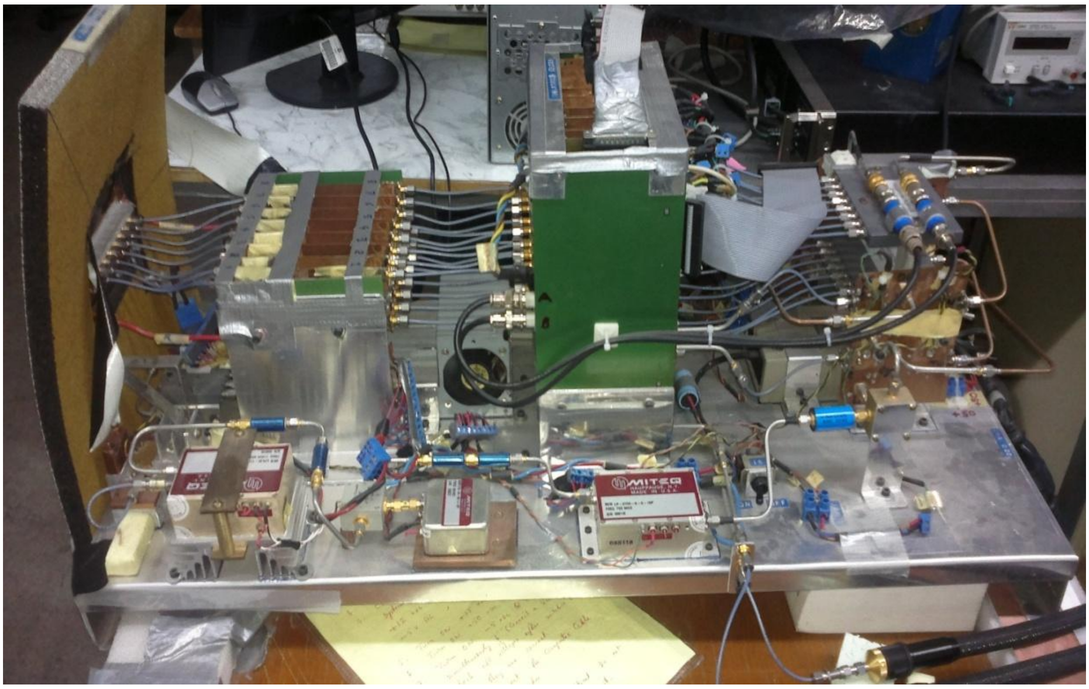

Figure 26. Receiver system architecture (side-view).

Eight signals coming from eight sub-arrays are down-converted to IF stage. Each down-converted signal is further divided into two signals: One goes to Channel-A complex vector modulator and the other signal goes to Channel-B complex vector modulator. There are 8 A (odd) channel vector modulator cards (identified with odd numbers 1, 3, 5, 7, 9, 11, 13, 15) and 8 B (even) channel vector modulator cards (identified with even numbers 2, 4, 6, 8, 10, 12, 14, 16). Following the vector modulators, 8 Channel-A and Channel-B signals are combined separately. In experimental studies, these combined outputs of Channel-A and Channel-B are used. For the MEP and REV methods, both outputs are monitored via Agilent E5071C Network Analyzer since a phase reference is required for those measurements. The phase is referenced to the B-output and associated vector modulator states have not been changed in CW operation.

In the experimental system, an X-band horn antenna is used as the transmitter and it is located at the far-field of the receive antenna array. Since the largest dimension of the array is 17 centimeters and with respect to Rayleigh formula,

$$R = 2 \times \frac{D^2}{\lambda}$$

Corresponding far field distance is calculated as 2.2 metres.

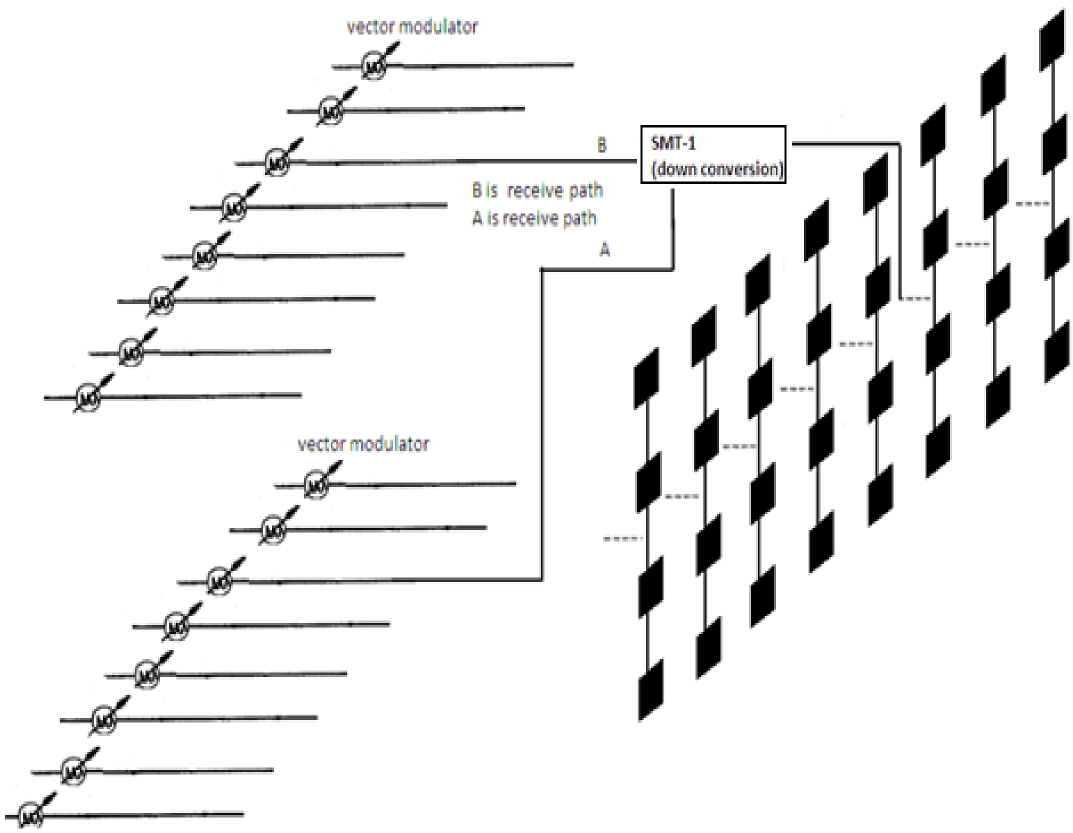

Figure 27. Schematic diagram of the phased array receiver showing Channel-A (odd VM cards) and Channel-B (even VM cards).

The transmitter horn is shown in **Figure 28** and overall experimental setup is presented in **Figure 29**.

Figure 28. Transmitter horn used in calibration measurements.

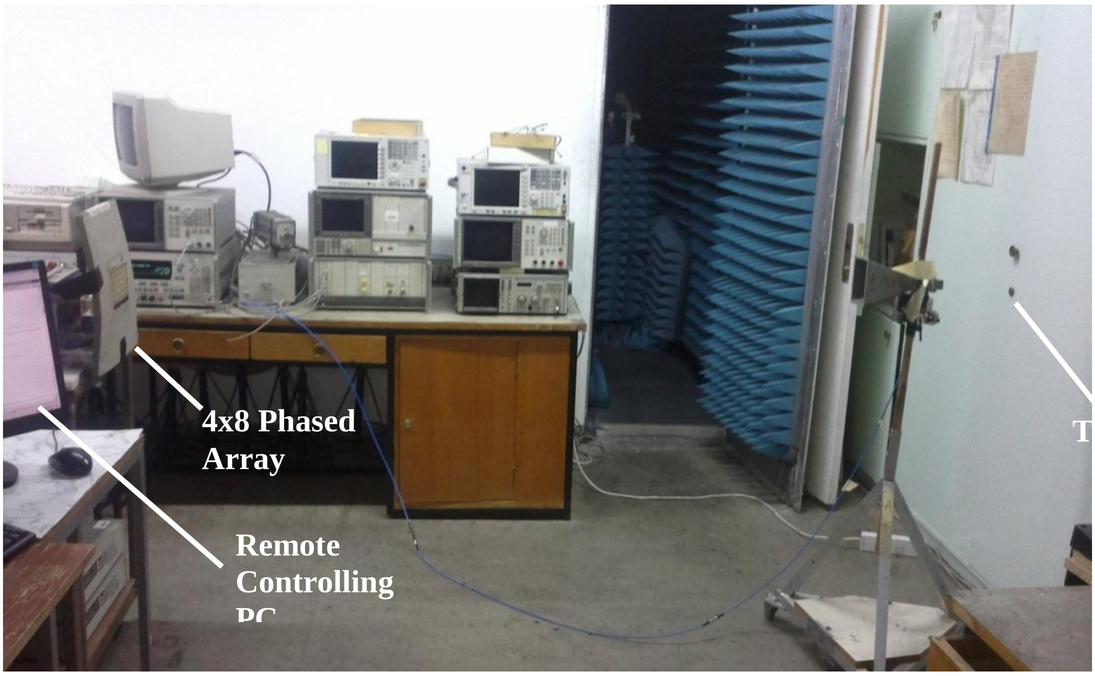

Figure 29. Experimental system (side-view).

The control of the state machine is commanded by parallel port bit stream compiled in C++. The required commands for implementing both REV and MEP procedures are automated by doing batch processing. Measurements are taken while ENA SERIES E5071C Network Analyzer is on the receive mode. The internal RF source is turned off for only receiving from A and B channels of the sample phased array antenna. The resultant data are obtained with automatic data acquisition of the Network Analyzer.

The phased array antenna use vector modulator cards. The phase shift is generated by the digital and analog attenuators. The vector modulator includes 90° 3dB hybrid at the fore, two pole phase modulator follows 3dB hybrid, analog and digital attenuators are placed after phase modulator and there is 0° combiner at the end. The coming signal is divided into two at first and these two signals with the 90° phase difference are attenuated properly to give certain phase shift after combination.

The experiments are performed both in the closed laboratory environment and at the terrace site of the Electric-Electronic Engineering Department. The weather conditions and environment conditions have effects on the performance and characteristic of the Phased Array Antenna system.

4.2 REV METHOD RESULTS

The measurements are performed both indoor and outdoor environments for REV method with different configurations of which results are stated and commented in this subsection.

The REV method measurements include all the effects such as mutual coupling between elements and cables, and also scattering effects induced by nearby objects. 45° phase steps are used while performing REV in measurements.

The probe is located far enough (2.2 m ; Rayleigh distance at 11.45 GHz) to radiate power to the whole array.

The REV results are presented by two measurement sets: The first part describes the results of odd card measurements and the second part describes the characterization of even cards.

In the first part of REV measurements, results of classic REV measurements obtained using only power measurements are used as correction data to calibrate test set-up. Only phase calibration, only amplitude calibration, both phase and amplitude calibrations are implemented to the test set-up. Moreover, measurements are repeated for three different days with same settings to observe effects of environmental conditions.

In the second part of REV measurements, two different configurations are used while taking measurements. In the first configuration, the tested element is only active while other seven elements are fully attenuated. In the second configuration, elements rather than tested element are active in their 1st phase states. Furthermore, in the second part of REV measurements, additional phase information is used to verify REV results up to some extent. Additional information is provided by channel-B (odd cards).

4.2.1 FIRST SET OF REV MEASUREMENTS

The first set of measurements was performed outside at the terrace site of EEMB D-building in order to minimize the effect of nearby scatterers on acquired data. The REV method is implemented using Agilent E5071C ENA for data acquisition and corrections were made for odd vector modulator cards. Results are normalized with respect to the second tested element for convenience.

Using 45° phase increments, the REV method yielded the following normalized excitation coefficients for the eight odd elements which are shown in **Table 11**:

Table 11. REV result in terms of excitation coefficients for eight odd cards

MAGNITUDE	1.46	1.00	1.08	0.76	0.70	0.79	0.78	1.08
ANGLE(DEG)	9	0	37	15	-30	-17	-50	-33

Described measurement was repeated on three different days using the same settings except for phase offset corrections which are performed with respect to [9 0 37 15 -30 -17 -50 -33] degrees set in the **Table 11** via the vector modulators. The excitation coefficients in those cases were determined as in **Table 12**:

Table 12. Three phase calibrated result sets corresponding to three days

DAY 1	MAGNITUDE	1.30	1.00	1.27	0.82	0.79	0.74	1.09	1.26
	ANGLE (DEG)	1.04	0.00	1.58	1.38	-2.20	-10.23	-0.80	-0.63
DAY 2	MAGNITUDE	1.38	0.99	1.22	0.84	0.81	0.71	1.01	1.27
	ANGLE (DEG)	2.66	0.00	1.67	5.83	-0.33	-5.36	2.13	0.65
DAY 3	MAGNITUDE	1.45	1.00	1.21	0.82	0.80	0.74	1.03	1.31
	ANGLE (DEG)	0.17	0.00	-8.85	0.66	-11.04	-19.29	-5.85	-9.45

Following a correction only in the amplitudes of the excitation by operating the vector modulators on their real axes, the REV procedure gave the following coefficients shown in **Table 13**:

Table 13. Amplitude calibrated data

MAGNITUDE	0.89	1.00	1.00	0.95	1.03	0.88	0.93	0.94
ANGLE(DEG)	15.1	0.0	22.7	9.1	-46.4	-48.6	-78	-54.5

A final trial with both amplitude and phase correction set by the respective vector modulators results in **Table 14**:

Table 14. Both amplitude and phase corrected data

MAGNITUDE	0.98	1.00	0.79	0.70	0.79	0.95	0.73	0.95
ANGLE(DEG)	7.1	0.0	20.6	-10.3	16.9	7.8	12.0	31.2

Due to the non-ideal vector modulator operation, it was discovered in the experiments that applied attenuation affected the inserted phase value and vice versa. It was because of the fact that applied phase and amplitude corrections did not completely eliminate the variations among the element excitations. Nevertheless, applied corrections determined by the REV method managed to confine the amplitude/phase variations within acceptable bounds.

4.2.2 SECOND SET OF REV MEASUREMENTS

Second set of REV measurements were performed indoors, in the sufficiently large open-space of the Microwave and Antenna Laboratory of EEMB. For these measurements, excitations for the even cards were altered while combined output of the odd cards was employed as the phase reference.

Configuration-I

For Configuration-I within the second set of REV measurements, only the tested element was kept active. This was achieved by applying full attenuation (44 dB) to the non-rotating elements in Channel-A through their respective vector modulators. The phase reference is taken as combined Channel-B output.

As for the first experiment in Configuration-I, recorded amplitude variation of the tested element (obtained by rotating the tested element's phase) was averaged for each element and those mean quantities were normalized with respect to that of 5^{th} element for convenience. **Table 15** lists obtained normalized mean amplitudes for each tested element. Since the reference component is negligible in this case, assuming perfect vector modulator operation, the reported values should correspond to excitation voltage amplitude of each element.

Table 15. Normalized average amplitudes of the tested elements in Channel-A (Configuration-I).

CARD NO	1	2	3	4	5	6	7	8
MAGNITUDE	1.66	1.42	1.56	1.30	1.00	1.12	1.57	1.87

The second experiment in Configuration-I is a slightly modified version of the first one in that complex voltage of each element was extracted for its 1° phase state. **Table 16** lists those complex quantities normalized with respect to that of the 5th element.

Table 16. Normalized complex voltage for each tested element in Channel-A at 1° phase state (Configuration-I).

CARD NO	1	2	3	4	5	6	7	8
MAGNITUDE	1.63	1.44	1.46	1.21	1.00	1.25	1.60	1.85
ANGLE(DEG)	-39.2	-26.5	-60.0	-32.7	0.0	0.7	29.3	17.6

Figure 30.(a)-(h) plot the measured complex voltage variation for each tested element when the REV procedure is applied with phase increments of 22.5°. Also overlaid on those plots are the ideal complex voltage variations, where the ideal voltage magnitude was determined by the average of absolute values of 16 measurements for each rotating element and the center points are taken as the origin (since there is no reference component in this case).

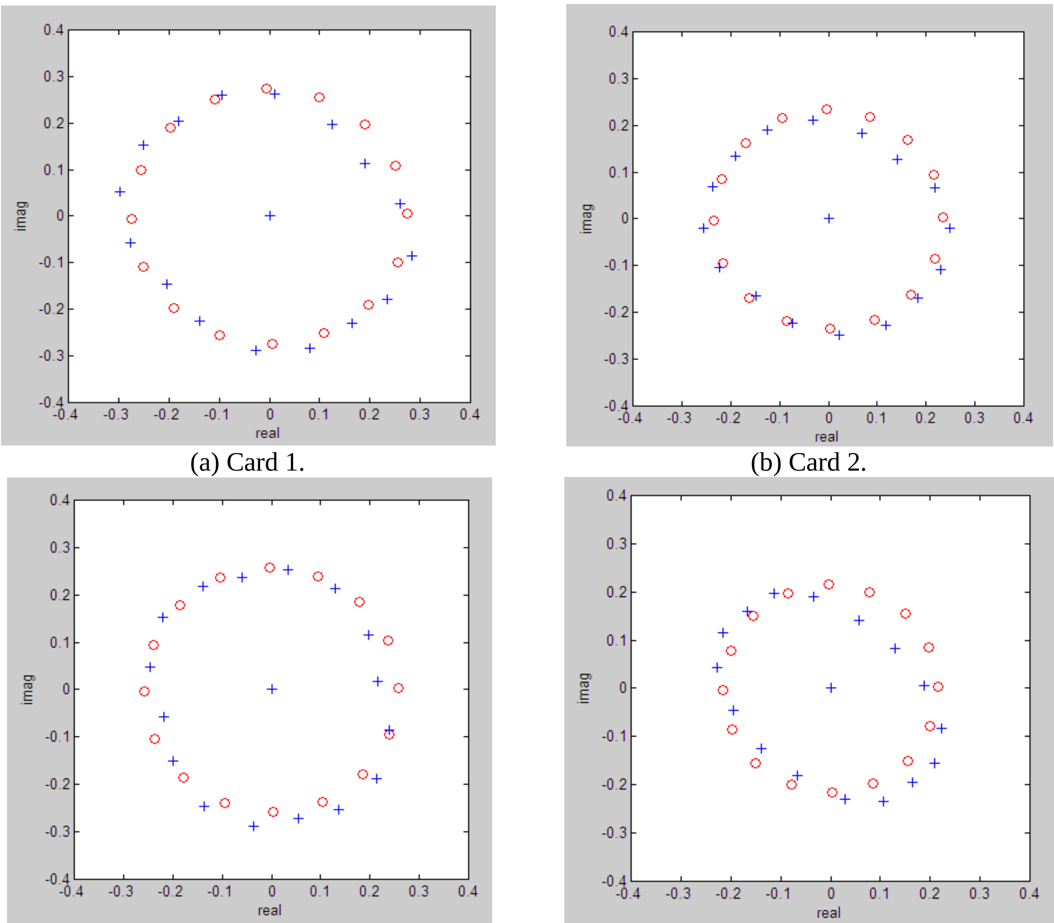

(a) Card 1. (b) Card 2.

(c) Card 3. (d) Card 4.

Figure 30. Complex voltage variation of each tested element measured using 22.5° phase increments (in Configuration-I). Ideal voltage variations are also overlaid on each plot with red circles. The origin and measured values are indicated with blue plus signs.

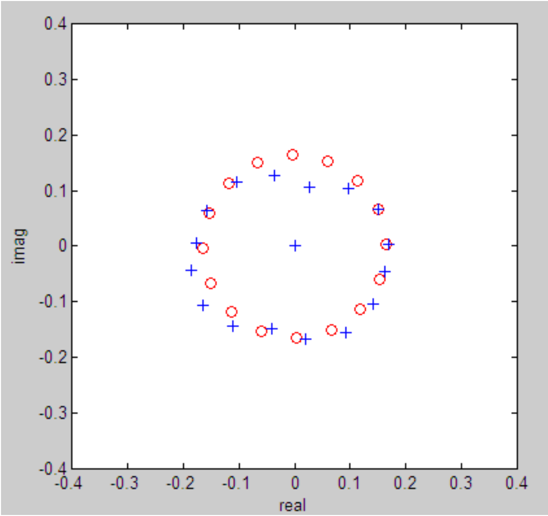

(e) Card 5.

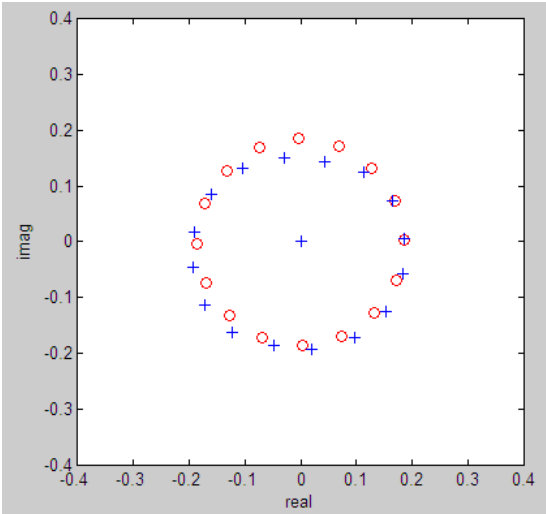

(f) Card 6.

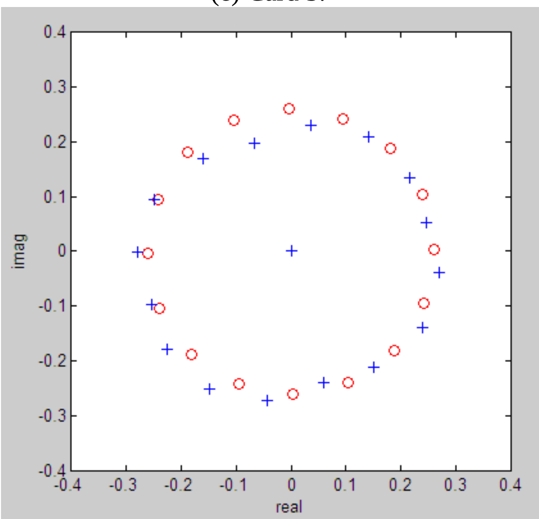

(g) Card 7.

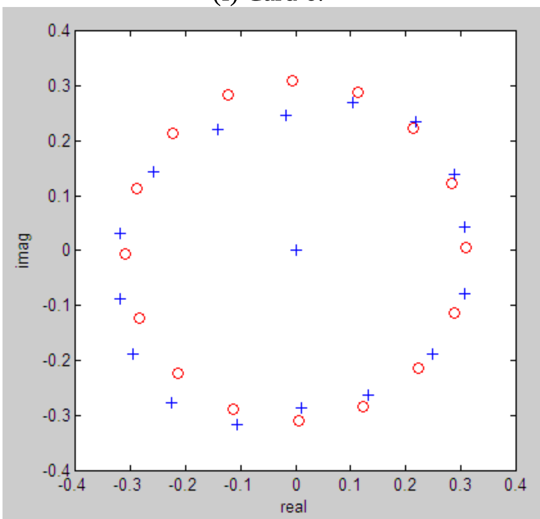

(h) Card 8.

Figure 30. (cont'd). Complex voltage variation of each tested element measured using 22.5° phase increments (in Configuration-I). Ideal voltage variations are also overlaid on each plot with red circles. The origin and measured values are indicated with blue plus signs.

The original REV method makes use of measured power (scalar instead of vector) quantities and a well-defined reference component. In Configuration-I, however, this reference component was effectively eliminated. Nevertheless, the original REV method was also applied to the experimental amplitude data and complex excitation coefficients of each element was extracted subsequently. **Table 17** tabulates these coefficients. It is observed from **Table 17** that there exists a correlation in the extracted excitation data with that of **Table 16** (in particular, phase values follow a similar trend). This latter observation suggests that there exists a nonzero reference component for the Configuration-I type experiments. Probable causes of this nonzero reference component are non-ideal vector modulator operation (actual applied attenuation might not be high enough) and/or leakage from Channel-B.

Table 17. Extracted excitation coefficients of eight elements using the original REV method (Configuration-I).

CARD NO	1	2	3	4	5	6	7	8
MAGNITUDE	1.66	1.42	1.56	1.31	1.00	1.12	1.57	1.87
ANGLE(DEG)	-34.7	-45.0	-86.4	-61.7	0.0	-13.9	20.7	17.0

In our test setup, the relative phase between A and B channels is known and this can be used as an advantage to improve the results of the original REV method. Since the original REV method requires a well-defined reference component, improvement of the reference component translates to greater confidence in the extracted element excitations. In order to test this idea experimentally, measured signals of Channel-A and Channel-B were combined as vectors and reference vector was increased in amplitude. Upon the application of the original REV method on this latter data set, the excitation coefficients listed in **Table 18** are obtained.

Table 18. Extracted excitation coefficients of eight elements using the original REV method (Configuration-I, reference component is increased in amplitude by vector addition of Channel-A and B data).

CARD NO	1	2	3	4	5	6	7	8
MAGNITUDE	1.51	1.36	1.32	1.22	1.00	1.04	1.45	1.76
ANGLE(DEG)	-36.7	-27.3	-64.0	-26.1	0.0	-2.5	25.8	15.1

An examination of **Table 15** and **Table 17** reveals that presented data using two different approaches are identical in magnitude. Consequently, the original REV method is noted to give correct mean values in general. Moreover, a comparison between **Table 16** and **Table 18** shows that the outcome of the original REV method employing a larger reference component agrees better with the initial phase differences of elements at their 1° states.

Although presented results are generally compatible with each other, it must be stated that imperfection of the phased array components (notably the vector modulators) affects the implementation of the REV procedure since applied phase increments are not that accurate and attenuation/inserted phase cannot be controlled that independently.

<u>Configuration- II</u>

As an alternative measurement case to Configuration-I, REV measurements were also conducted with the non-tested elements in Channel-A kept at their initial states (with their vector modulators set to 0 dB attenuation and 1° insertion phase) instead of turning those off. This measurement scenario is termed Configuration-II and the experiments described in this section adopt this scheme. Similar with the Configuration-I, the phase reference is taken as the combined output of Channel-B.

Using the additional phase information in our experiments as an advantage over the original REV method, received signals for each phase-rotated element were acquired first and those complex voltages were then processed to identify and remove the reference component from those. Hence, resulting data set features negligible reference component and the amplitude averaging step outlined in the previous section can then be applied. When this is done, the mean excitation amplitudes Channel-A elements are obtained as listed in **Table 19**.

Table 19. Normalized average amplitudes of the tested elements in Channel-A (Configuration-II, reference component is removed by using the additional phase information).

CARD NO	1	2	3	4	5	6	7	8
MAGNITUDE	1.71	1.45	1.58	1.33	1.00	1.12	1.58	1.90

There seems to be a good agreement between the mean excitation amplitudes tabulated in **Table 19** and that of **Table 15**. This observation suggests that our experimental system indeed yields stable results for two different measurement configurations.

Extracted excitations of phase-rotated Channel-A elements for their 1° states are listed in **Table 20**. This list serves as a reference for the initial phase differences between elements, as the indicated magnitude data in **Table 20** are not accurate (since these values are obtained by extracting the reference component from the measured value of first state of phase-rotated element).

Table 20. Normalized complex voltage for each tested element in Channel-A at 1° phase state (Configuration-II).

CARD NO	1	2	3	4	5	6	7	8
MAGNITUDE	1.78	1.63	1.73	1.20	1.00	1.28	1.80	2.14
ANGLE(DEG)	-42.9	-30.1	-67.8	-31.5	0.0	0.6	29.7	19.1

There is a good agreement between the excitation phase data of elements tabulated in **Table 16** and **Table 20.** This observation once again justifies the stability of the experimental setup for two different measurement configurations.

For the sake of completeness, REV measurement results for Configuration-II are presented in **Figure 31.(a)-(h)**, which explicitly demonstrate the phase-rotation concept and show the direct (reference) component present in the measurements (which is a generated by the active non-phase-rotated elements in Channel-A).

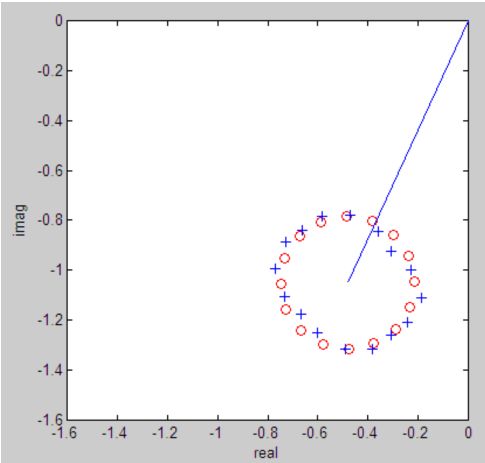

(a) Card 1.

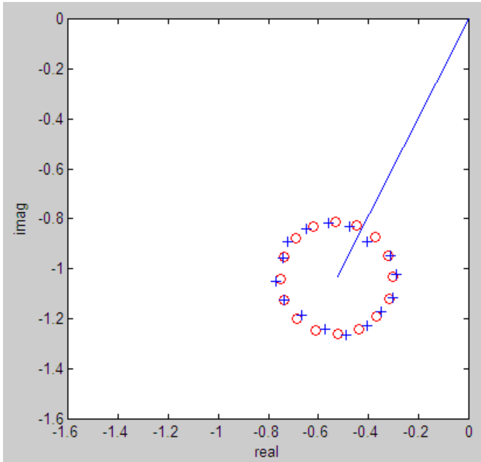

(b) Card 2.

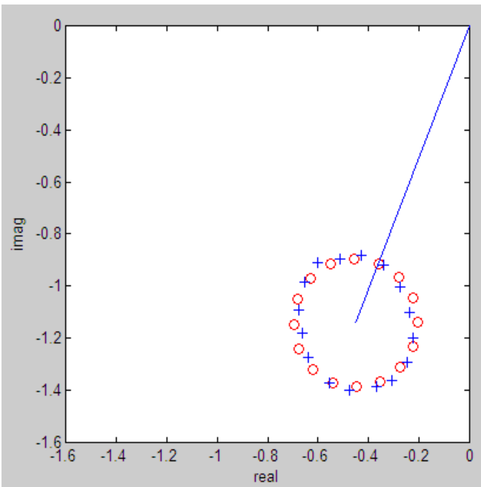

(c) Card 3.

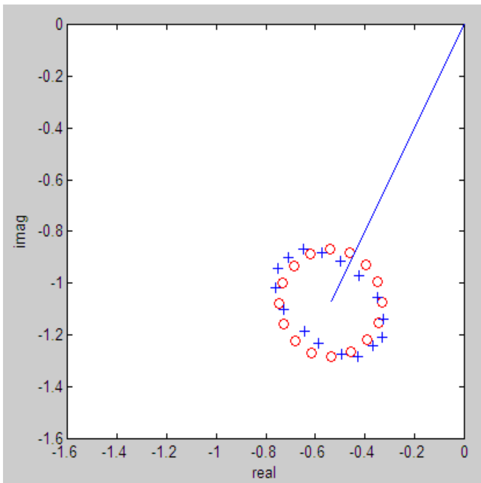

(d) Card 4.

Figure 31. Complex voltage variation of each tested element measured using 22.5° phase increments (in Configuration-II). Ideal voltage variations are also overlaid on each plot with red circles. Measured quantities are indicated with blue plus signs, the direct (reference) component is depicted as blue lines.

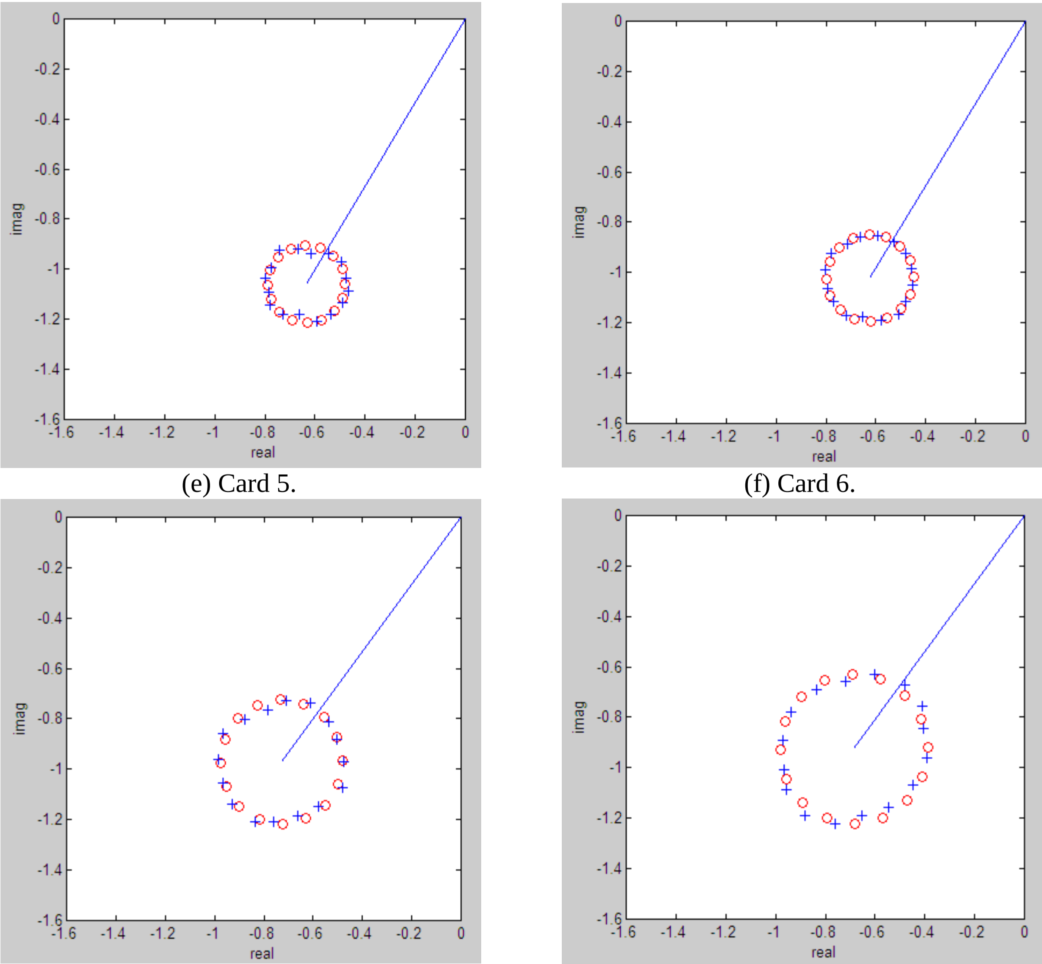

(e) Card 5. (f) Card 6.

(g) Card 7. (h) Card 8.

Figure 31. (cont'd) Complex voltage variation of each tested element measured using 22.5° phase increments (in Configuration-II). Ideal voltage variations are also overlaid on each plot with red circles. Measured quantities are indicated with blue plus signs, the direct (reference) component is depicted as blue lines.

Proceeding similarly with Configuration-I type experiments, the original REV method was also applied to the measurement data using only the amplitude information. The corresponding excitation data for the eight elements are listed in **Table 21**. Reported phase data are noted to agree with the ones tabulated in **Table 20**, yet the agreement can be improved further as explained shortly.

Table 21. Extracted excitation coefficients of eight elements using the original REV method (Configuration-II).

CARD NO	1	2	3	4	5	6	7	8
MAGNITUDE	1.64	1.41	1.68	1.11	1.00	1.16	1.73	2.16
ANGLE(DEG)	-56.7	-37.7	-85.8	-54.8	0.0	-3.0	32.2	24.2

As an improvement to the original REV method, an alternative algorithm is proposed which seeks to eliminate the residual systematic errors present in the REV procedure in an iterative fashion: Any component different from the fixed component in measurements of all elements is subtracted and added as its new version to the reference component and results are re-calculated. The proposed method can be defined as an improved version of the evaluation procedure found in the literature. It must be emphasized that no phase or reference component information is required for the proposed approach.

Table 22 lists the evaluated excitations of eight elements with the proposed REV algorithm using only measured power values. It can be seen that phase difference values in **Table 22** and that for first states of elements in **Table 20** agree more closely compared to the results obtained using the original REV method directly (**Table 21**). These findings serve to highlight the potential of the proposed REV method in terms of its improved antenna calibration accuracy.

Table 22. Extracted excitation coefficients of eight elements using the proposed iterative REV algorithm (Configuration-II).

CARD NO	1	2	3	4	5	6	7	8
MAGNITUDE	1.64	1.41	1.68	1.11	1.00	1.16	1.73	2.16
ANGLE(DEG)	-48.9	-33.2	-74.7	-49.1	0.0	3.0	26.1	17.2

In the section of REV measurements, it is seen that REV method can be applied to the experimental set-up and a number of configurations can be implemented using REV algorithm. Implemented different configurations show that REV method is available to develop and accuracy level can be increased by using additional information.

In the first set of REV measurements, only power measurements are used as the classic REV method and amplitude, phase corrections are performed by using the extracted values handled with the classic REV method. Reduction in errors to make array elements identical is seen clearly in both only phase and only amplitude corrections in the first set of REV measurements. Moreover, although operation of vector modulator is non-ideal, result of REV with both amplitude and phase corrections implemented version proves that calibration is done. Repeated measurements show that environmental conditions can be effective in measurements since measurements are different from each other although there is no significant change in weather conditions.

In second set of REV measurements, there is no significant change in results of configuration 1 and configuration 2 with respect to other elements being active or fully attenuated. By the use of additional phase information, electric field vectors corresponding to power measurements in REV procedure are shown in the second set of REV measurements. Moreover, iterative REV procedure which is proposed in this work reduces phase error as it can be shown in the second set of REV measurements.

4.3 MEP METHOD RESULTS

As opposed to REV method, the MEP method measures received signal of each element simultaneously, i.e. all elements are tested at the same time in a systematic manner. In order to achieve this, a four-bit system was realized by the experimental setup and sixteen combined signals were measured in accordance with the MEP procedure.

In REV method part, a 3-bit phase shifter is used by using 45° phase increments. In the MEP, 22.5° phase steps are used. The MEP procedure is implemented to odd cards of experimental set-up and results of implementations are normalized with respect to the second element. Two successive phase corrections are performed to observe the convergence of error after calibration. Moreover, MEP method is implemented to the even cards in the laboratory to check consistence of REV and MEP methods in terms of magnitude and angle since REV method is implemented to even cards in laboratory environment.

Procedure of the MEP method is implemented on odd vector modulator cards and results for 8 sub-arrays are normalized with respect to second sub-array are represented in **Table 23**,

Table 23. MEP results normalized with respect to the second element

MAGNITUDE	1.34	1.00	0.99	0.89	0.77	0.66	1.03	1.18
ANGLES	6.54°	0.00°	-18.9°	4.0°	52.0°	58.5°	73.83°	77.23°

Angle values are in the range from -19 to 77 degrees in **Table 23**.

MEP results are presented in **Table 24 after phase calibration** with respect to corrections of MEP result before calibration above (-6° 0° 19° -4° -52° -58° -74° -77°);

Table 24. MEP results calibrated with respect to phase offsets in **Table 23**.

MAGNITUDE	0.8	1.0	1.27	0.81	0.80	0.69	1.14	1.20
ANGLES	-12.8°	0.0°	-17°	-21°	-26.1	-5.5°	2.8°	-17.9°

Angle values lie in the range from -26 to 3 degrees in **Table 24**.

MEP results after phase calibration with respect to corrections of MEP result after first phase calibration (13° 0° 17° 21° 26° 5° -3° 18°) are shown in **Table 25**;

Table 25. MEP results calibrated with respect to deficiencies in **Table 24**.

MAGNITUDE	0.9	1.00	0.92	0.73	0.70	0.76	0.96	1.10
ANGLES	6.0°	0.00°	-2.74°	-5.7°	11.1°	-1.9°	4.4°	5.6°

Angle values lie in the range from -6 to 11 degrees in **Table 25**.

Table 26 presents the unnormalized excitation coefficients which are calculated with the MEP method for even cards of eight subarrays.

Figure 32 and **Figure 33** provide a comparison of the (unnormalized) element excitation coefficients calculated with the REV (with Configuration-II) and MEP methods. It is observed from those plots that there exists good agreement between these extracted quantities (both in magnitude and phase), an observation which serves to crosscheck successful operation of each method. From those plots, a slight discrepancy is noted for the complex voltage of the 5th element. This slight difference is most probably caused by the violation of the equal phase increment assumption of the MEP method (which in turn is due to the imperfect vector modulator operation).

Table 26. Unnormalized excitation coefficients of the eight even channels calculated with the MEP method.

CARD NO	1	2	3	4	5	6	7	8
MAGNITUDE	1.71	1.4	1.57	1.24	0.74	1.00	1.51	1.83
ANGLE(DEG)	-46.8	-31.2	-68.4	-39.2	15.0	6.7	34.7	26.7

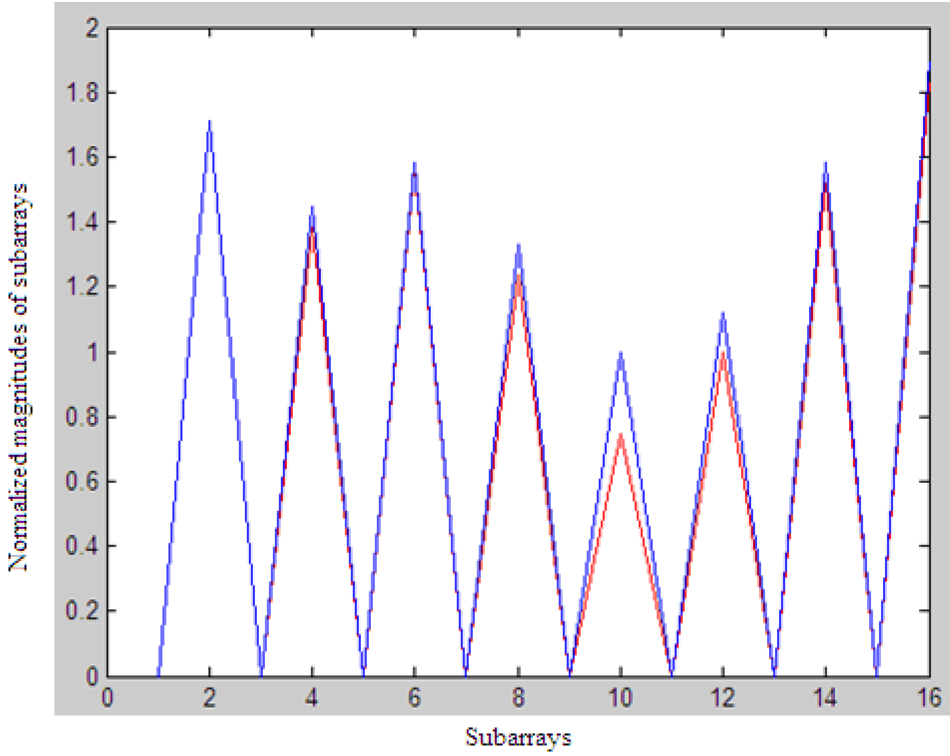

Figure 32. Magnitude values for the excitations of subarrays calculated with MEP (red) and REV (blue) methods (All values are normalized with respect to fifth element in REV).

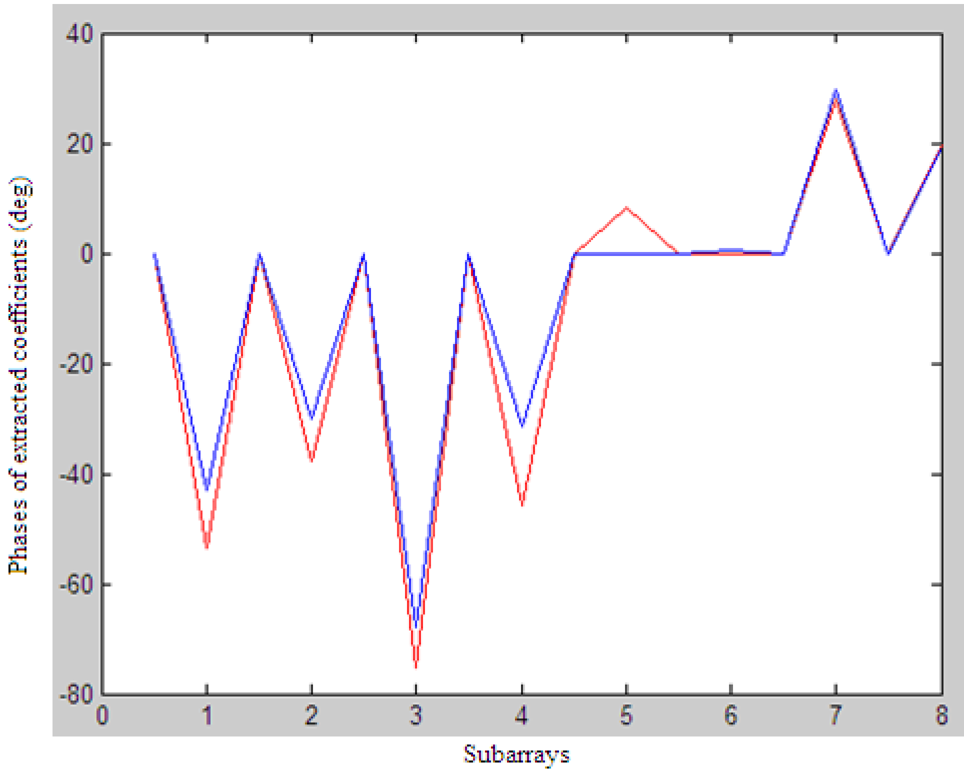

Figure 33. Phase values for the excitations of subarrays calculated with MEP (red) and REV (blue) methods.

In the MEP measurements, according to results of two successive phase corrections in **Table 24** and **Table 25**, it is seen that the phase errors converge to a narrower interval which shows the success of implemented MEP method in **Figure 34**. In the chapter-3, phase correction for the OSMA was shown in **Figure 21**, comparation between experimental work in this thesis and similar work in the literature shows that MEP method is successful to reduce differences in initial phases of elements.

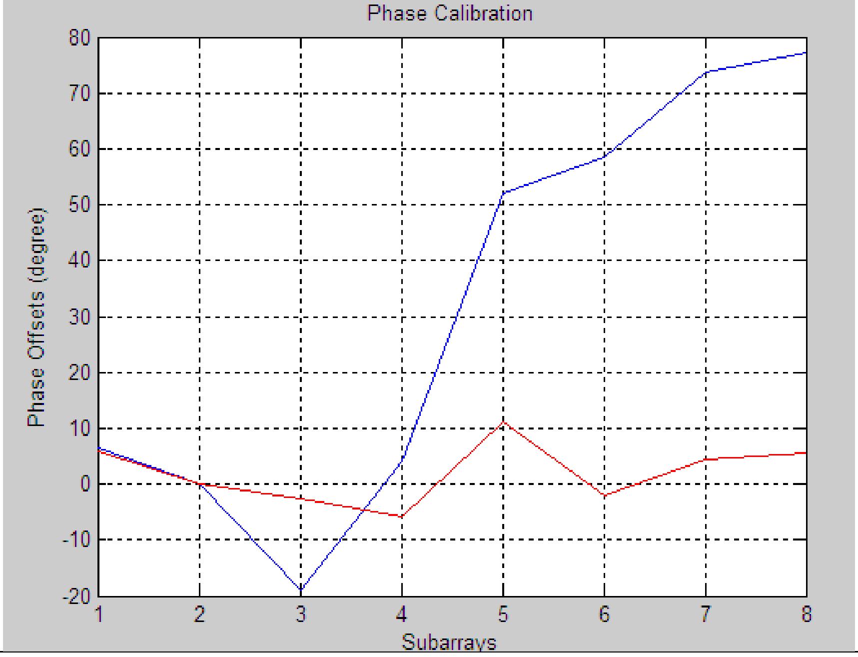

Figure 34. Phase calibration using MEP method

MEP method is a time efficient method since 16 measurements are required to extract eight correction coefficients corresponding to excitation values of eight subarrays by the use of four-bit phase shifter. On the other hand, REV method requires 64 measurements to get correction coefficients for eight subarrays.

In REV and MEP methods, phase shifters of individual elements should have stable phase increments while rotating phases of elements. This rule is a stricter requirement in MEP method since Fourier transform is used to extract excitations of elements and Fourier transform clarifies excitation of elements according to their phase increments. In the REV method, errors in certain phase increments can be compensated by increasing measurements since there is a circle fitting algorithm to the samples of measurements.

Moreover, MEP method procedure has certain steps such as increasing phases of elements with different specific phase increments, using phase information to take measurements and taking Fourier transform. On the other hand, it is seen in the process of experimental work that implementation of REV method is more flexible than implementation of MEP method. Phase increments in REV method can be decided according to the time concern. Furthermore, REV method can be expanded by the use of additional information such as phase information. The use of additional phase information brings additional system requirements but such an additional information increases reliability of REV method and may also be used as a verification way to the implementation of REV method.

At the end of the experimental work, it is inferred that although REV and MEP methods are different from each other, these two methods are suitable to be used at the same time in a Phased Array Antenna system since they both need to stable phase shifters and location of the external antenna dedicated to calibration is same for REV and MEP while applying these methods to an antenna array.

CHAPTER 5

CONCLUSION

The calibration of a Phased Array Antenna system is very vital to sustain the achieved performance of the system. In the literature, there are many suggested calibration methods and configurations. In this thesis, a general literature survey about calibration of PAA systems is provided. As a result of this literature search, nine calibration methods are listed and explained with their implementation procedures, constraints, weaknesses and strengths. Two of these calibration methods are selected from the cited nine methods, namely; REV method and MEP method.

Both REV and MEP methods use an external fixed transmitter antenna which is located at the phase center axis of the tested array. The distance between the external antenna and the array under test is determined by Rayleigh formula providing far field conditions. The REV and MEP methods can be also implemented in radiating near field; however, distance coefficients and additional phase terms should be considered.

In this thesis, an X-band phased array antenna receiver system is used as the experimental test set-up and an X-band horn antenna is used as the transmitter. Measurements are performed on the roof of the EEMB D-building and in the Microwave and Antenna Laboratory. Moreover, measurements with the same configuration and settings are repeated in different days and under different weather conditions to see the stability in the results of REV and MEP methods.

REV method is simulated by using MATLAB® and simulation results take place in the thesis to explain procedure of the method better. An iterative way is generated to improve the classical REV method removing the necessity of using larger references which is an important constraint for the implementation of the REV method. Furthermore, Experimental measurements are performed by a number of different configurations to see the performance of the method in the scope of this thesis.

Simulations of the other selected method MEP are also presented in this thesis. Experimental measurements are taken for the MEP method and results are listed. Moreover, measurement results for the MEP and REV method is compared and convenience between two methods is observed.

The MEP method is a very time-efficient calibration method since a number of array elements can be calibrated simultaneously. On the other hand, constant phase shifts are required while taking signals which give correction factors of elements. Therefore, to use the MEP method, stable and checked phase shifters have to be used.

The REV method uses only power measurements and gives data including both magnitude and phase of the tested element with respect to a fixed reference. On the other hand, the MEP method utilizes both magnitude and phase information. Therefore, the REV method can be implemented more easily to an existing PAA system since the need to additional phase information in the MEP method requires more complexity.

Furthermore, the REV method is more accurate than the MEP method, however; REV method takes much time compared to the MEP method. It should be noticed that the REV and the MEP methods can be used together to calibrate the system. For such an operation, the REV method can be implemented for periodic calibration which is performed at long time intervals and the MEP method can be implemented at shorter time intervals. Moreover, calibration way can be chosen as the REV method and the MEP method can be used for verification.

As the future work, the planar implementation of the REV and MEP methods by a pick-up probe in the plane of the array should be investigated. Disadvantages of the use of the external antenna in front of the array can be removed by the planar implementation and it should be seen whether additional benefits can be achieved or not.

Moreover, quality of implemented calibration method should be known to complete the cycle of calibration. Therefore, algorithms to handle the quality of calibration method should be investigated as a future work.

Better calibration search will continue as long as the effort to get better performance from the phased array antenna system exists.

REFERENCES

[1] G.A. Hampson, A.B. Smolders, "A Fast and Accurate Scheme for Calibration of Active Phased-Array Antennas", IEEE APS Symposium, Orlando USA, 1999.

[2] G. A. Hampson, J.G. de Vaate, "Initial Calibration and Beamforming Results from the Thousand Element Phased-Array", IEEE, 2001.

[3] B. Smolders, G.A. Hampson "Deterministic WF Nulling in Phased Arrays for the Next Generation of Radio Telescopes", IEEE Antenna's and Propagation Magazine, August 2002.

[4] K.M. Lee, R.S. Chu and S.C. Liu "A Built-in Performance-Monitoring/Fault Isolation and Correction (PM/FIC) System for Active Phased Array Antennas", IEEE Transactions on Antennas & Propagation, AP-41 , pp. 1530-1540, 1993.

[5] M. Goris, G.A Hampson, A. Joseph and F.M.A. Smits, "An Adaptive Beamforming System for Radio Frequency Interference Rejection", IEE Proceedings on Radar, Sonar and Navigation, vol.146, no.2, pp. 73-77, 2002.

[6] A. Smolders and G. Kant, "System Specification THEA" *SKA* Memo: Reference www.astron.nl/ska April 11, 1999, last visited at December, 2010.

[7] G. Hampson, "Calibration of the RF Beamformer Vector Modulators", Internal ASTRON Report. November 23 2000, Available: www.astron.nl/-hampson/publlc.html**,** last visited at December, 2010.

[8] A. van Ardenne, F.M.A. Smits, "Technical Aspects for the Square Kilometer Array Interferometer," Proceedings of the ESTEC Workshop on Large Antennas in Radio Astronomy, The Netherlands**,** WPP-I 10, pp. 117-127, February 1996.

[9] X.F. Zheng, T. Gao, X.L. Chen, "Mid-field Calibration Technique of Active Phased Array Antennas", IEEE, 2005.

[10] A. Agrawal, A. Jablon, "A Calibration Technique for Active Phased Array Antennas", IEEE International Symposium on Phased Array Systems and Technology, pp. 223–228, 2003.

[11] M. Sarcione, *et al*, "The Design, Development and Testing of the THAAD (Theater High Altitude Area Defense) Solid State Phased Array (formerly Ground Based Radar)", 1996 IEEE Int. Symp. On Phased Array Systems and Technology, pp. 260-265, 1996.

[12] K. Weese, DITZINGEN (DE), "Calibration Method for Smart Antenna Arrays", Patent No: US 7593826 B2, Date of Patent: Sep. 22, 2009.

[13] A.M. Shitikov, A.V.Bondarik, "Multi-Element PAA Calibration with REV Method", *Antenna Theory and Techniques, 2003. 4th International Conference on*, vol.2, no., pp. 761-764 vol.2, 9-12 Sept. 2003.

[14] Y. Matsumoto, I. Yamazaki, S. Hama, "Calibration Method of Mutual Coupling in Beam Forming Network for Phased-Array Antennas", Electronics and Communications in Japan, Part 2, vol.84, no.1, 2001, Scripta Technica, 2000.

[15] S. Mano, T. Katagi, "A Method for Measuring Amplitude and Phase of Each Radiating Element of a Phased Array ". Electronics and Communication in Japan (IECE), vol. 65-B, no.5, pp. 58-64, May 1982.

[16] A.G. Shubov, A.V.Shishlov, "Analysis of Method for Phased Array Antenna Phasing Based on Amplitude Measurements Only", Proceedings of the XXVIII Moscow International Conference on Antenna Theory and Technology, pp.295-298, 22-24 September 1998.

[17] M. Liu, Z. Feng, "Combined REV Method for Near-Field Calibration of Phased Array Antenna" IEEE/ICMMT, 18-21 April 2007.

[18] N. Kojima, K. Shiramatsu, I. Chiba, T. Ebisui, N.Kurihara, "Measurement and Evaluation Techniques for an Airborne Active Phased Array Antenna", 1996 IEEE International Symposium on Phased Array Systems and Technology, pp 231 – 236, October 1996.

[19] R. Yonezawa, Y. Konishi, I. Chiba, T. Katagi, "Beam-shape Correction in Deployable Phased Arrays", IEEE Trans. Antennas and Propagation, vol. 47, no.3, pp. 482 – 486, March 1999.

[20] I.J. Gupta, et al, "An Experimental Study of Antenna Array Calibration", IEEE Trans. Antennas Propag., vol.51, no.3, pp. 664-667, 2003.

[21] J. Pierre, M. Kaveh, “Experimental Performance of Calibration and Direction-Finding Algorithms,” in Proc. IEEE ICCASP, Toronto, Canada, pp. 1365–1368, May 1991.

[22] B.C. Ng and C.M.S. See, “Sensor-array Calibration using a Maximum Likelihood Approach”, IEEE Trans. Antennas Propagat., vol. 44, pp. 827–835, June 1996.

[23] A.J. Weiss and B. Friedlander, “Array Shape Calibration using Eigenstructure Methods,” in Proc. 23rd Asilmor Conf. Signals, Systems, and Computing, Pacific Grove, CA, pp. 925–929, 1989.

[24] Y. Matsumoto, I. Yamazaki, S. Hama, “Calibration Method of Mutual Coupling in Beam Forming Network for Phased-Array Antennas”, Electronics and Communications in Japan, Part 2, vol.84, no.1, 2001, Scripta Technica, 2000.

[25] Y. Matsumoto, T. Ide, M. Tanaka, T. Orikasa, Y. Yamasa, “Array Element and BFN Design for Phased-Array-fed Satellite Antennas”, 17^{th} AIAA ICSS Conf, AIAA-98- 1224, 1998.

[26] M. Tanaka, *et al*, “On Orbit Measurement of Phased Arrays in Satellites by Rotating Element Electric Field Vector Method”, Electronics and Communications in Japan (Part I: Communications), vol.81, no.1, pp. 1-13, 1998.

[27] C. Shipley, D. Woods, “Mutual Coupling-Based Calibration of Phased Array Antennas” IEEE, 2000.

[28] H.M. Aumann, A.J. Fenn, F.G. Willwerth, “Phased Array Antenna Calibration and Pattern Prediction Using Mutual Coupling Measurements”, IEEE Trans. Antennas Propagation, vol.37, no.7, pp. 844-850, July 1989.

[29] Y. Neidman, R. Shavit, A. Bronshtein, “Diagnostic of Phased Arrays with Fault Elements Using the Mutual Coupling Method”, IET Microw. Antennas Propag., vol. 3, Iss. 2, pp. 235–241, 2009.

[30] D.L. Collinson, LAFAYETTE, NY(US), “Mutual Coupling Method for Calibrating a Phased Array”, Patent No: US 7362266 B2, Date of Patent : Apr. 22, 2008.

[31] R.E. MILLER, MT LAUREL, NJ(US), R.M. REESE, Philadelphia, PA(US), “Structure for an Array Antenna, and Calibration Method Therefor” , Patent No: US 6356233 B1, Date of Patent : March. 12, 2002.

[32] A. Hızal et al., “TÜBİTAK COST-260 Projesi Adaptif Anten Dizileri Final Raporu”, 2002.